



MOX–Report No. 13/2014

**Supremizer stabilization of POD-Galerkin approximation of parametrized Navier-Stokes equations**

BALLARIN, F.; MANZONI, A.; QUARTERONI, A.; ROZZA, G.

MOX, Dipartimento di Matematica “F. Brioschi”  
Politecnico di Milano, Via Bonardi 9 - 20133 Milano (Italy)

[mox@mate.polimi.it](mailto:mox@mate.polimi.it)

<http://mox.polimi.it>



# SUPREMIZER STABILIZATION OF POD-GALERKIN APPROXIMATION OF PARAMETRIZED NAVIER-STOKES EQUATIONS

FRANCESCO BALLARIN<sup>1</sup>, ANDREA MANZONI<sup>2</sup>, ALFIO QUARTERONI<sup>1,3</sup>, AND GIANLUIGI ROZZA<sup>2</sup>

**ABSTRACT.** In this work we present a stable proper orthogonal decomposition (POD)-Galerkin approximation for parametrized steady Navier-Stokes equations. The stabilization is guaranteed by the use of supremizers solutions that enrich the reduced velocity space. Numerical results show that an equivalent inf-sup condition is fulfilled, yielding stability for both velocity and pressure. Our stability analysis is first carried out from a theoretical standpoint, then confirmed by numerical tests performed on a parametrized two-dimensional backward facing step flow.

## 1. INTRODUCTION AND MOTIVATIONS

Several applications in physics or engineering need an efficient solution of parametrized partial differential equations (PDEs); this necessitates the computation of the solution of (possibly nonlinear) PDEs for several different “scenarios”. A solution by traditional methods like finite elements or finite volumes may not always be feasible. In general, reduced-order models (ROMs) are devised to deliver an accurate solution at lower computational costs. For nonlinear PDEs several issues need however to be faced in order to guarantee efficiency, accuracy and reliability, also when using ROMs. These include the efficient exploration of the parameters space to build reduced basis spaces that, ideally, should: *(i)* have low dimension but also the capability to capture fine physical features; *(ii)* be stable also for noncoercive problems as in the case of saddle-point problems; *(iii)* allow accurate and fast estimation of stability factors, as recently pointed out in [1, 2].

POD was born to provide efficient model order reduction in turbulent viscous flow computations, with the aim of preserving the most important energetic flow features. POD is based on modal analysis and singular value decomposition [3, 4, 5, 6]. Several further improvements have been addressed in the subsequent studies; these includes eigenproblems solving, error estimation, physical parametrization not only restricted to the temporal variable, optimal sampling, etc., see e.g. [7, 8, 9, 10, 11, 12, 13]. On the other hand, Reduced Basis (RB) methods were proposed for nonlinear viscous flows since the Eighties [14], whereas important theoretical contributions and many new methodological developments were provided in more recent years [15, 16, 17, 18], including the application to new unconventional fields [19, 20]. In recent years, growing attention has been dedicated to the combination of Galerkin strategies with POD [21, 22, 23] and to stabilization techniques both for POD [24, 25, 9, 26] and RB methods [27, 28, 29, 30].

The aim of this work is to use the RB framework in its state of the art formulation for the stable and accurate approximation of flows in a POD setting, in order to improve the performance of this latter. In this way, POD could benefit from a previously developed robust framework for the RB stabilization of viscous flows that can also allow a correct pressure recovery. In this work we test such a method on nonlinear steady viscous flows modelled by Navier-Stokes equations

<sup>1</sup> MOX - Modeling and Scientific Computing, Dipartimento di Matematica, Politecnico di Milano, P.zza Leonardo da Vinci 32, I-20133 Milano, Italy, [francesco.ballarin@polimi.it](mailto:francesco.ballarin@polimi.it)

<sup>2</sup> SISSA MathLab, International School for Advanced Studies, via Bonomea 265, I-34136 Trieste, Italy, [amanzoni@sissa.it](mailto:amanzoni@sissa.it), [grozza@sissa.it](mailto:grozza@sissa.it)

<sup>3</sup> CMCS - Modelling and Scientific Computing, Ecole Polytechnique Fédérale de Lausanne, Station 8, CH-1015 Lausanne, Switzerland, [alfio.quarteroni@epfl.ch](mailto:alfio.quarteroni@epfl.ch)

*Key words and phrases.* proper orthogonal decomposition; reduced basis method; pressure stabilization; equivalent inf-sup condition; parametrized Navier-Stokes equations.

and characterized by both physical and geometrical parametrization. In the offline stage of the resulting strategy, several Navier-Stokes truth solutions are computed, and a POD is performed to extract a low dimensional representation of both velocity and pressure spaces. However, either when we aim to obtain an online approximation of the pressure field, or when we consider geometrical parameters, the reduced velocity space needs to be properly enriched by the so-called supremizers, and a POD procedure needs to be applied also on these functions. Finally, an online Galerkin projection over this enriched space can be performed online, in order to get a reduced-order approximation of both velocity and pressure fields. The proposed method offers a valid approach preserving offline-online computational decomposition procedures, stability, and all the properties inherited by POD (such as orthonormalized basis functions for a robust algebraic stability, and hierarchical spaces construction), strengthened by the ones offered by Galerkin projection (best fit approximation). At the same time, such a POD-Galerkin approach could provide an alternative option to greedy algorithms for systems where error bounds are not yet available or to integrate already developed numerical codes more easily in the reduced framework. A detailed analysis of the role of supremizer enrichment in the POD-Galerkin context is then performed, showing some criteria for an efficient enrichment both by means of theoretical considerations and numerical examples.

In the next Section steady parametrized Navier-Stokes problems and their full-order approximation are introduced, considering both physical and geometrical parameters. In Section 3 a POD-Galerkin ROM is presented. The usual offline-online decomposition is required; a POD is used for basis construction, and enrichment of the velocity space by means of supremizers is performed. Section 4 provides a stability analysis for the POD-Galerkin ROM, as well as the description of the supremizer enrichment strategy. Some heuristic criteria ensuring a very efficient enrichment procedure are described in Section 5. Numerical results dealing with parametrized backward facing step flows are given in Section 6. Finally, some conclusions follow in Section 7.

## 2. FORMULATION AND FULL-ORDER APPROXIMATION OF PARAMETRIZED NAVIER-STOKES EQUATIONS

In this paper we focus on the efficient solution of parametrized steady Navier-Stokes (NS) equations, because of their ubiquitous role in fluid flows applications. Whenever possible, we will favor the description of our POD-based ROM using an algebraic formalism.

**2.1. Continuous formulation.** In the steady case, on a spatial domain  $\Omega(\boldsymbol{\mu}_g) \subset \mathbb{R}^d$ ,  $d = 2, 3$ , NS equations read as follows:

$$\begin{cases} -\nu(\boldsymbol{\mu}_p)\Delta\boldsymbol{u} + (\boldsymbol{u} \cdot \nabla)\boldsymbol{u} + \nabla p = \boldsymbol{f}(\boldsymbol{\mu}_p) & \text{in } \Omega(\boldsymbol{\mu}_g), \\ \operatorname{div} \boldsymbol{u} = 0 & \text{in } \Omega(\boldsymbol{\mu}_g), \\ \boldsymbol{u} = \boldsymbol{g}_D(\boldsymbol{\mu}_p) & \text{on } \Gamma_D, \\ \boldsymbol{u} = \boldsymbol{0}, & \text{on } \Gamma_W(\boldsymbol{\mu}_g), \\ \nu(\boldsymbol{\mu}_p)\frac{\partial \boldsymbol{u}}{\partial \boldsymbol{n}} - p\boldsymbol{n} = \boldsymbol{g}_N(\boldsymbol{\mu}_p), & \text{on } \Gamma_N, \end{cases} \quad (1)$$

for some given distributed force term  $\boldsymbol{f}$ , Dirichlet data  $\boldsymbol{g}_D$  and Neumann fluxes  $\boldsymbol{g}_N$ . Here we denote by  $\boldsymbol{\mu} = (\boldsymbol{\mu}_g, \boldsymbol{\mu}_p)^T \in \mathcal{D} \subset \mathbb{R}^P$  a vector of parameters which may characterize either the geometrical configuration  $\Omega(\boldsymbol{\mu}_g)$  or physical properties of our system, such as dynamical viscosity  $\nu = \nu(\boldsymbol{\mu}_p)$ , boundary data  $\boldsymbol{g}_D = \boldsymbol{g}_D(\boldsymbol{\mu}_p)$ ,  $\boldsymbol{g}_N = \boldsymbol{g}_N(\boldsymbol{\mu}_p)$  or source terms  $\boldsymbol{f} = \boldsymbol{f}(\boldsymbol{\mu}_p)$ . For the sake of notation, we shall distinguish between  $n_p$  physical parameters  $\boldsymbol{\mu}_p \in \mathcal{D}_p \subset \mathbb{R}^{n_p}$  and  $n_g = P - n_p$  geometrical parameters  $\boldsymbol{\mu}_g \in \mathcal{D}_g \subset \mathbb{R}^{n_g}$ . We thus denote by  $(\boldsymbol{u}, p) = (\boldsymbol{u}(\boldsymbol{\mu}), p(\boldsymbol{\mu}))$  the velocity and pressure fields, by omitting the dependence on  $\boldsymbol{\mu}$  for the sake of notation.

We denote by  $\Gamma_W$  and  $\Gamma_D$  the portion of  $\partial\Omega$  where we impose homogeneous (resp., inhomogeneous) Dirichlet conditions, whereas we assign on  $\Gamma_N = \partial\Omega \setminus (\Gamma_W \cup \Gamma_D)$  the Neumann conditions; here  $\boldsymbol{n}$  denotes the normal unit vector to  $\Gamma_N$ . Hereafter we assume that  $\Gamma_D$  and  $\Gamma_N$  are not affected by the geometrical parametrization of the domain: this simplifies our problem, by avoiding the use of Piola transformation even in presence of geometrical parametrizations

[31]. For the sake of simplicity, we consider the case  $\mathbf{f} = \mathbf{g}_N = \mathbf{0}$ ; the extension to other cases is straightforward. We also define the Reynolds number as  $Re = L|\bar{\mathbf{u}}|/\nu$ , being  $L$  a characteristic length of the domain,  $\bar{\mathbf{u}}$  a typical velocity of the flow and  $\nu$  the kinematic viscosity; in the numerical test cases presented we will consider flows with  $Re \in [1, 10^3]$ .

To derive the algebraic formulation of (1), we first need to write this problem under weak form. To do this, we introduce a reference,  $\boldsymbol{\mu}_g$ -independent configuration  $\Omega$ , by assuming that each parametrized domain  $\Omega(\boldsymbol{\mu}_g)$  can be obtained as the image of  $\Omega$  through a parametrized map  $T(\cdot; \boldsymbol{\mu}_g) : \mathbb{R}^d \rightarrow \mathbb{R}^d$ , i.e.  $\Omega(\boldsymbol{\mu}_g) = T(\Omega; \boldsymbol{\mu}_g)$ . Moreover, we denote by  $V, Q$  the velocity and the pressure space, respectively, defined over  $\Omega$ ; here

$$V = \mathbf{H}_{0,\Gamma_E}^1(\Omega), \quad Q = L^2(\Omega)$$

being  $\Gamma_E = \Gamma_D \cup \Gamma_W$ . We equip  $V$  and  $Q$  with the (vector)  $H^1$ -seminorm and the  $L^2$ -norm, the former being equivalent to the  $H^1$ -norm since  $\Gamma_E \neq \emptyset$ . Bold symbols denote vectorial functions in the velocity space. The weak formulation can be obtained by multiplying (1) for test functions  $(\mathbf{v}, q)$  and integrating by parts; then, we trace everything back onto the reference domain  $\Omega$ . In this way, we end up with the following weak parametrized formulation of (1): find<sup>1</sup>  $(\mathbf{u}, p) \in V \times Q$  such that

$$\begin{cases} a(\mathbf{u}, \mathbf{v}; \boldsymbol{\mu}) + b(\mathbf{v}, p; \boldsymbol{\mu}) + c(\mathbf{u}, \mathbf{u}, \mathbf{v}; \boldsymbol{\mu}) + d(\mathbf{u}, \mathbf{v}; \boldsymbol{\mu}) = F(\mathbf{v}; \boldsymbol{\mu}) & \forall \mathbf{v} \in V \\ b(\mathbf{u}, q; \boldsymbol{\mu}) = G(q; \boldsymbol{\mu}) & \forall q \in Q \end{cases} \quad (2)$$

where

$$a(\mathbf{u}, \mathbf{v}; \boldsymbol{\mu}) = \int_{\Omega} \frac{\partial \mathbf{u}}{\partial x_i} \kappa_{ij}(\mathbf{x}; \boldsymbol{\mu}) \frac{\partial \mathbf{v}}{\partial x_j} d\mathbf{x}, \quad b(\mathbf{v}, q; \boldsymbol{\mu}) = - \int_{\Omega} q \chi_{ij}(\mathbf{x}; \boldsymbol{\mu}) \frac{\partial v_j}{\partial x_i} d\mathbf{x} \quad (3)$$

are the bilinear forms related to diffusion and pressure/divergence operators, respectively, whereas

$$c(\mathbf{u}, \mathbf{v}, \mathbf{z}; \boldsymbol{\mu}) = \int_{\Omega} u_i \chi_{ji}(\mathbf{x}; \boldsymbol{\mu}) \frac{\partial v_m}{\partial x_j} w_m d\mathbf{x} \quad (4)$$

is the trilinear form related to the convective term. We adopt the convention of summation over repeated indices. Here we denote by

$$\begin{aligned} \kappa(\mathbf{x}; \boldsymbol{\mu}) &= \nu(\boldsymbol{\mu}_p)(J_T(\mathbf{x}; \boldsymbol{\mu}_g))^{-1}(J_T(\mathbf{x}; \boldsymbol{\mu}_g))^{-T}|J_T(\mathbf{x}; \boldsymbol{\mu}_g)| \\ \chi(\mathbf{x}; \boldsymbol{\mu}) &= (J_T(\mathbf{x}; \boldsymbol{\mu}_g))^{-1}|J_T(\mathbf{x}; \boldsymbol{\mu}_g)|, \end{aligned} \quad (5)$$

the tensors encoding both physical and geometrical parametrizations in the NS operators;  $J_T \in \mathbb{R}^{d \times d}$  is the Jacobian matrix of the map  $T(\cdot; \boldsymbol{\mu}_g)$ , and  $|J_T|$  its determinant. Other terms are devised by the lifting of the Dirichlet boundary conditions: denoting by  $\mathbf{l}(\boldsymbol{\mu}_p)$  a parametrized lifting function such that  $\mathbf{l}(\boldsymbol{\mu}_p)|_{\Gamma_D} = \mathbf{g}_D(\boldsymbol{\mu}_p)$ ,  $\mathbf{l}(\boldsymbol{\mu}_p)|_{\Gamma_W} = \mathbf{0}$ , we have that

$$\begin{aligned} d(\mathbf{u}, \mathbf{v}; \boldsymbol{\mu}) &= c(\mathbf{l}(\boldsymbol{\mu}_p), \mathbf{u}, \mathbf{v}; \boldsymbol{\mu}) + c(\mathbf{u}, \mathbf{l}(\boldsymbol{\mu}_p), \mathbf{v}; \boldsymbol{\mu}) \\ F(\mathbf{v}; \boldsymbol{\mu}) &= -a(\mathbf{l}(\boldsymbol{\mu}_p), \mathbf{v}; \boldsymbol{\mu}) - c(\mathbf{l}(\boldsymbol{\mu}_p), \mathbf{l}(\boldsymbol{\mu}_p), \mathbf{v}; \boldsymbol{\mu}), \quad G(q; \boldsymbol{\mu}) = -b(\mathbf{l}(\boldsymbol{\mu}_p), q; \boldsymbol{\mu}). \end{aligned}$$

In particular, we consider parametrized Dirichlet data  $\mathbf{g}_D(\boldsymbol{\mu}_p) = \Theta_D(\boldsymbol{\mu}_p)\tilde{\mathbf{g}}$ , for a given scalar function  $\Theta_D(\boldsymbol{\mu}_p)$  and a suitable inlet profile  $\tilde{\mathbf{g}}$ . Thus, a parameter independent lifting function  $\tilde{\mathbf{l}}$  is actually computed in practice, and  $\mathbf{l}(\boldsymbol{\mu}_p) = \Theta_D(\boldsymbol{\mu}_p)\tilde{\mathbf{l}}$ . Without loss of generality, we can take a divergence-free  $\tilde{\mathbf{l}}$ , e.g. considering a suitably scaled velocity of a Stokes flow, so that  $G(q; \boldsymbol{\mu}) = 0$ .

---

<sup>1</sup>We denote, with a little abuse of notation, the solution on the reference domain still by  $(\mathbf{u}, p)$ . Hereafter however we will refer only to this solution, so that no confusion arises (with the exception of the plots in Figures 4, 5 and 10 which are drawn on the deformed domain and adding the lifting for a better comparison).

**2.2. The full-order model and its algebraic formulation.** To formulate the full-order model, we introduce two finite-dimensional subspaces  $V_h \subset V$ ,  $Q_h \subset Q$  of dimension  $N_{\mathbf{u}}^h$  and  $N_p^h$ , respectively, being  $h > 0$  related to the computational mesh size. We consider a Galerkin-Finite Element (FE) approximation, denote by  $\{\varphi_i^h\}_{i=1,\dots,N_{\mathbf{u}}^h}$  and  $\{\zeta_k^h\}_{k=1,\dots,N_p^h}$  two (Lagrangian) basis of the FE spaces. The Galerkin-FE approximation of the parametrized problem (2) reads as follows: given  $\boldsymbol{\mu} \in \mathcal{D}$ , we seek for (the full-order solution)  $(\mathbf{u}_h(\boldsymbol{\mu}), p_h(\boldsymbol{\mu})) \in V_h \times Q_h$  such that

$$\left\{ \begin{array}{ll} a(\mathbf{u}_h(\boldsymbol{\mu}), \mathbf{v}_h; \boldsymbol{\mu}) + d(\mathbf{u}_h(\boldsymbol{\mu}), \mathbf{v}_h; \boldsymbol{\mu}) + b(\mathbf{v}_h, p_h(\boldsymbol{\mu}); \boldsymbol{\mu}) \\ \quad + c(\mathbf{u}_h(\boldsymbol{\mu}), \mathbf{u}_h(\boldsymbol{\mu}), \mathbf{v}_h; \boldsymbol{\mu}) = F(\mathbf{v}_h; \boldsymbol{\mu}) & \forall \mathbf{v}_h \in V_h \\ b(\mathbf{u}_h(\boldsymbol{\mu}), q_h; \boldsymbol{\mu}) = G(q_h; \boldsymbol{\mu}) & \forall q_h \in Q_h. \end{array} \right. \quad (6)$$

For algebraic purposes, let us state the following bijection between  $\mathbb{R}^{N_{\mathbf{u}}^h}$  and  $V_h$  (resp.  $\mathbb{R}^{N_p^h}$  and  $Q_h$ ):

$$\left\{ \begin{array}{ll} \underline{\mathbf{v}} = (v_h^{(1)}, \dots, v_h^{(N_{\mathbf{u}}^h)})^T \in \mathbb{R}^{N_{\mathbf{u}}^h} & \leftrightarrow \quad \mathbf{v}_h = \sum_{r=1}^{N_{\mathbf{u}}^h} v_h^{(r)} \varphi_r^h \in V_h, \\ \underline{\mathbf{q}} = (q_h^{(1)}, \dots, q_h^{(N_p^h)})^T \in \mathbb{R}^{N_p^h} & \leftrightarrow \quad q_h = \sum_{r=1}^{N_p^h} q_h^{(r)} \zeta_r^h \in Q_h. \end{array} \right. \quad (7)$$

Thanks to this identification, (6) is equivalent to the following (nonlinear) system:

$$\begin{bmatrix} A(\boldsymbol{\mu}) + C(\underline{\mathbf{u}}(\boldsymbol{\mu}); \boldsymbol{\mu}) & B^T(\boldsymbol{\mu}) \\ B(\boldsymbol{\mu}) & 0 \end{bmatrix} \begin{bmatrix} \underline{\mathbf{u}}(\boldsymbol{\mu}) \\ \underline{\mathbf{p}}(\boldsymbol{\mu}) \end{bmatrix} = \begin{bmatrix} \underline{\mathbf{f}}(\boldsymbol{\mu}) \\ \underline{\mathbf{g}}(\boldsymbol{\mu}) \end{bmatrix} \quad (8)$$

for the vector of coefficients  $\underline{\mathbf{u}} = (u_h^{(1)}, \dots, u_h^{(N_{\mathbf{u}}^h)})^T$ ,  $\underline{\mathbf{p}} = (p_h^{(1)}, \dots, p_h^{(N_p^h)})^T$  where, for  $1 \leq i, j \leq N_{\mathbf{u}}^h$  and  $1 \leq k \leq N_p^h$ :

$$\begin{aligned} (A(\boldsymbol{\mu}))_{ij} &= a(\varphi_j^h, \varphi_i^h; \boldsymbol{\mu}) + d(\varphi_j^h, \varphi_i^h; \boldsymbol{\mu}), & (B(\boldsymbol{\mu}))_{ki} &= b(\varphi_i^h, \zeta_k^h; \boldsymbol{\mu}), \\ (C(\underline{\mathbf{u}}(\boldsymbol{\mu}); \boldsymbol{\mu}))_{ij} &= \sum_{m=1}^{N_{\mathbf{u}}^h} u_m^{(m)}(\boldsymbol{\mu}) c(\varphi_m^h, \varphi_j^h, \varphi_i^h; \boldsymbol{\mu}), \end{aligned} \quad (9)$$

$$(\underline{\mathbf{g}}(\boldsymbol{\mu}))_k = -b(\mathbf{l}_h, \zeta_k^h; \boldsymbol{\mu}), \quad (\underline{\mathbf{f}}(\boldsymbol{\mu}))_i = -a(\mathbf{l}_h, \varphi_i^h; \boldsymbol{\mu}) - c(\mathbf{l}_h, \mathbf{l}_h, \varphi_i^h; \boldsymbol{\mu}) \quad (10)$$

and  $\mathbf{l}_h = \mathbf{l}_h(\boldsymbol{\mu}_p) \in V_h$  is a FE interpolant of the lifting function. Moreover, let us introduce the mass matrices  $X_{\mathbf{u}}$ ,  $X_p$  for the velocity and pressure spaces, respectively, whose elements are given by

$$(X_{\mathbf{u}})_{ij} = (\varphi_j^h, \varphi_i^h)_V \quad (X_p)_{kl} = (\zeta_l^h, \zeta_k^h)_Q$$

for  $1 \leq i, j \leq N_{\mathbf{u}}^h$  and  $1 \leq k, l \leq N_p^h$ , being  $(\cdot, \cdot)_V$  and  $(\cdot, \cdot)_Q$  the (discrete) inner products defined over the two spaces. Moreover, we denote (with a little abuse of notation) by

$$(\underline{\mathbf{v}}, \underline{\mathbf{w}})_V = (X_{\mathbf{u}} \underline{\mathbf{v}}, \underline{\mathbf{w}}), \quad (\underline{\mathbf{p}}, \underline{\mathbf{q}})_Q = (X_p \underline{\mathbf{p}}, \underline{\mathbf{q}})$$

the corresponding vector inner products for velocity and pressure fields, respectively; here  $(\cdot, \cdot)$  denotes the usual Euclidean inner product in  $\mathbb{R}^{N_h}$  ( $N_h = N_{\mathbf{u}}^h, N_p^h$  depending on the case).

Solving the NS system (8) requires a nonlinear iteration with a linearized problem (involving nonsymmetric, indefinite matrix) being solved at each step; Newton and fixed-point (or Picard) iterations are the most common strategies. Here we consider the latter, since the radius of the ball of convergence of Newton's method is typically proportional to the viscosity  $\nu$ , and better initial guesses would be needed as the Reynolds number increases [32].

**2.3. A key assumption for efficient ROMs: affine parametric dependence.** In order to deal with efficient ROMs, we need to ensure a further assumption on the operators appearing in (9)-(10), already at the full-order level. The key requirement for an efficient ROM evaluation is the capability to decouple the construction stage of the reduced-order space (offline) from the parametric evaluation stage (online), thus featuring the so-called Offline/Online decomposition. To meet this goal, we require that matrices and vectors appearing in (9)-(10) fulfil the assumption of affine parametric dependence, so that they can be written, e.g., as

$$A(\boldsymbol{\mu}) = \sum_{q=1}^{Q_A} \Theta_q^A(\boldsymbol{\mu}) A^q, \quad C(\underline{\mathbf{w}}; \boldsymbol{\mu}) = \sum_{q=1}^{Q_C} \Theta_q^C(\boldsymbol{\mu}) C^q(\underline{\mathbf{w}}), \quad \underline{\mathbf{f}}(\boldsymbol{\mu}) = \sum_{q=1}^{Q_f} \Theta_q^f(\boldsymbol{\mu}) \underline{\mathbf{f}}^q,$$

and in a similar way for the other terms. This expression is straightforward to be obtained in case of (both physical and geometrical) affine parametrizations. Instead, when dealing with more general nonaffine parametrizations, an approximate affine expansion is usually recovered by means of the so-called empirical interpolation method (EIM) [33]. See e.g. [16] for further details.

Although this procedure may entail severe costs (in terms of CPU time and storing), this is mandatory in order to ensure an efficient evaluation of the POD-based ROM, for any parameter value. In fact, as we will see in Section 3, under this assumption it is possible to assemble the reduced-order operators during the Online stage by relying on  $(N_u^h, N_p^h)$ -independent algebraic structures, thus making each ROM query very efficient – and even more when dealing with nonlinear operators. Alternative strategies – yet related to a discrete empirical interpolation method (DEIM) – can also be employed, as shown e.g. in [34].

### 3. A POD-GALERKIN ROM FOR PARAMETRIZED NAVIER-STOKES EQUATIONS

In this section we present a POD-Galerkin ROM for solving parametrized NS equations based on a Proper Orthogonal Decomposition technique and a Galerkin projection. ROMs for solving parametrized PDEs are usually based upon a suitable and stable combination of “snapshot” FE solutions, thus aiming at building reduced spaces  $V_N \subset V_h$ ,  $Q_N \subset Q_h$  of global approximation functions, for velocity and pressure, respectively. At least two approaches in the construction stage of the reduced basis can be pursued: greedy algorithms and Proper Orthogonal Decomposition [1]. In this paper we consider this latter [26, 35, 36, 11].

When dealing with (possibly, unsteady) incompressible flows depending on physical parameters, several ROMs based on POD aim at approximating just the velocity fields. This is motivated by the fact that each snapshot is already divergence free, and so all the pressure terms in the momentum equation drop out (that is, the continuity equation is automatically fulfilled). However, we might be interested to get a reduced approximation of the pressure field too, either because of the application at hand, or since the divergence-free assumption fails to hold due to the geometrical variation/parametrization. In this case, the reduced model will benefit of a standard Galerkin projection with orthonormal global approximation basis functions for both velocity and pressure, provided a suitable stabilization is introduced to fulfil an equivalent inf-sup condition.

**3.1. A POD-Galerkin ROM for simultaneous approximation of velocity and pressure.** We will first derive the formulation of our POD-Galerkin ROM, leaving the inf-sup stabilization issue to the following section. In particular, we adopt an algebraic standpoint, by considering the following bijection between the spaces  $\mathbb{R}^{N_u}$  and  $V_N$  (resp.  $\mathbb{R}^{N_p}$  and  $Q_N$ ):

$$\begin{cases} \underline{\mathbf{v}}_N = (v_N^{(1)}, \dots, v_N^{(N_u)})^T \in \mathbb{R}^{N_u} & \leftrightarrow & v_N = \sum_{n=1}^{N_u} v_N^{(n)} \boldsymbol{\varphi}_n \in V_N, \\ \underline{\mathbf{q}}_N = (q_N^{(1)}, \dots, q_N^{(N_p)})^T \in \mathbb{R}^{N_p} & \leftrightarrow & q_N = \sum_{n=1}^{N_p} q_N^{(n)} \zeta_n \in Q_N. \end{cases} \quad (11)$$

Let us denote by  $\Xi = \{\boldsymbol{\mu}^1, \dots, \boldsymbol{\mu}^n\} \subset \mathcal{D}$  a (large) training sample of  $n$  points chosen randomly over  $\mathcal{D}$ , and consider the *snapshot matrices*

$$S_{\mathbf{u}} = [\underline{\mathbf{u}}(\boldsymbol{\mu}^1) \mid \dots \mid \underline{\mathbf{u}}(\boldsymbol{\mu}^n)] \in \mathbb{R}^{N_{\mathbf{u}}^h \times n}, \quad S_p = [\underline{\mathbf{p}}(\boldsymbol{\mu}^1) \mid \dots \mid \underline{\mathbf{p}}(\boldsymbol{\mu}^n)] \in \mathbb{R}^{N_p^h \times n};$$

here we take  $n < N_p^h$  since we assume to deal with a very fine FE discretization, where  $N_{\mathbf{u}}^h > N_p^h \gg 1$ . A POD basis for the velocity and pressure spaces can be obtained by considering the singular value decomposition (SVD) of the following matrices

$$X_{\mathbf{u}}^{1/2} S_{\mathbf{u}} = U_{\mathbf{u}} \Sigma_{\mathbf{u}} W_{\mathbf{u}}^T, \quad X_p^{1/2} S_p = U_p \Sigma_p W_p^T$$

where

- $U_{\mathbf{u}} \in \mathbb{R}^{N_{\mathbf{u}}^h \times N_{\mathbf{u}}^h}$  and  $U_p \in \mathbb{R}^{N_p^h \times N_p^h}$  are two orthogonal matrices of left singular vectors;
- $W_{\mathbf{u}} \in \mathbb{R}^{n \times n}$  and  $W_p \in \mathbb{R}^{n \times n}$  are two orthogonal matrices of right singular vectors;
- $\Sigma_{\mathbf{u}} \in \mathbb{R}^{N_{\mathbf{u}}^h \times n}$  and  $\Sigma_p \in \mathbb{R}^{N_p^h \times n}$  are two diagonal matrices, made by the *singular values* of  $S_{\mathbf{u}}$  and  $S_p$ , so that  $(\Sigma_{\mathbf{u}})_{ii} = \sigma_i^{\mathbf{u}}$  with  $\sigma_1^{\mathbf{u}} \geq \sigma_2^{\mathbf{u}} \geq \dots \geq \sigma_n^{\mathbf{u}} \geq 0$ ,  $(\Sigma_p)_{ii} = \sigma_i^p$  with  $\sigma_1^p \geq \sigma_2^p \geq \dots \geq \sigma_n^p \geq 0$ .

In fact, for any  $N_{\mathbf{u}}, N_p < n$ , the POD basis (of dimension  $N_{\mathbf{u}}, N_p$ ) is given by the first  $N_{\mathbf{u}}, N_p$  columns of  $U_{\mathbf{u}}, U_p$ , respectively (left singular vectors). In this way, we can define

$$Z_{\mathbf{u}} = [\underline{\varphi}_1 \mid \dots \mid \underline{\varphi}_{N_{\mathbf{u}}}] \in \mathbb{R}^{N_{\mathbf{u}}^h \times N_{\mathbf{u}}}, \quad Z_p = [\underline{\zeta}_1 \mid \dots \mid \underline{\zeta}_{N_p}] \in \mathbb{R}^{N_p^h \times N_p}$$

as the basis matrices for velocity and pressure, respectively. Thus, the basis functions of spaces  $V_N$  and  $Q_N$  are FE solutions, expressed w.r.t. a Lagrangian FE basis by the components of the columns of  $Z_{\mathbf{u}}, Z_p$ , respectively. An equivalent (and more efficient) approach considers the so-called *method of snapshots*. In this case, we shall solve two eigenproblems for the correlation matrices

$$C_{\mathbf{u}} = S_{\mathbf{u}}^T X_{\mathbf{u}} S_{\mathbf{u}} \in \mathbb{R}^{n \times n}, \quad C_p = S_p^T X_p S_p \in \mathbb{R}^{n \times n}$$

and define the POD bases for velocity and pressure spaces as their first  $N_{\mathbf{u}}$  (resp.  $N_p$ ) eigenvectors:

$$\underline{\varphi}_j = \frac{1}{\sqrt{\lambda_j^{\mathbf{u}}}} S_{\mathbf{u}} \underline{\psi}_j^{\mathbf{u}}, \quad \underline{\zeta}_l = \frac{1}{\sqrt{\lambda_l^p}} S_p \underline{\psi}_l^p, \quad j = 1, \dots, N_{\mathbf{u}}, \quad l = 1, \dots, N_p,$$

being

$$C_{\mathbf{u}} \underline{\psi}_j^{\mathbf{u}} = \lambda_j^{\mathbf{u}} \underline{\psi}_j^{\mathbf{u}}, \quad C_p \underline{\psi}_l^p = \lambda_l^p \underline{\psi}_l^p, \quad j = 1, \dots, N_{\mathbf{u}}, \quad l = 1, \dots, N_p$$

and  $\lambda_j^{\mathbf{u}} = (\sigma_j^{\mathbf{u}})^2$ ,  $\lambda_l^p = (\sigma_l^p)^2$ , respectively. Basis functions are automatically orthonormal, since

$$(\underline{\varphi}_i, \underline{\varphi}_j)_V = \frac{1}{\sqrt{\lambda_i^{\mathbf{u}} \lambda_j^{\mathbf{u}}}} (\underline{\psi}_i^{\mathbf{u}}, S_{\mathbf{u}}^T X_{\mathbf{u}} S_{\mathbf{u}} \underline{\psi}_j^{\mathbf{u}}) = \frac{1}{\sqrt{\lambda_i^{\mathbf{u}} \lambda_j^{\mathbf{u}}}} (\underline{\psi}_i^{\mathbf{u}}, \lambda_j^{\mathbf{u}} \underline{\psi}_j^{\mathbf{u}}) = \sqrt{\frac{\lambda_j^{\mathbf{u}}}{\lambda_i^{\mathbf{u}}}} \delta_{ij}, \quad (12)$$

$$(\underline{\zeta}_k, \underline{\zeta}_l)_Q = \frac{1}{\sqrt{\lambda_k^p \lambda_l^p}} (\underline{\psi}_k^p, S_p^T X_p S_p \underline{\psi}_l^p) = \frac{1}{\sqrt{\lambda_k^p \lambda_l^p}} (\underline{\psi}_k^p, \lambda_l^p \underline{\psi}_l^p) = \sqrt{\frac{\lambda_l^p}{\lambda_k^p}} \delta_{kl}. \quad (13)$$

We remark that the reduced spaces dimensions  $N_{\mathbf{u}}, N_p$  can be chosen as the smallest integers for which the “energy” of the retained modes

$$E^{\mathbf{u}}(\underline{\varphi}_1, \dots, \underline{\varphi}_{N_{\mathbf{u}}}) = \frac{\sum_{j=1}^{N_{\mathbf{u}}} (\sigma_j^{\mathbf{u}})^2}{\sum_{j=1}^n (\sigma_j^{\mathbf{u}})^2}, \quad E^p(\underline{\zeta}_1, \dots, \underline{\zeta}_{N_p}) = \frac{\sum_{l=1}^{N_p} (\sigma_l^p)^2}{\sum_{l=1}^n (\sigma_l^p)^2}$$

is greater than  $1 - \varepsilon_{tol}^*$ , for some prescribed (small) tolerance  $\varepsilon_{tol}^*$ .

**3.2. Algebraic formulation of the POD-Galerkin ROM.** As shown in the previous subsection, by performing a POD over each set of velocity and pressure snapshots, we manage to obtain two orthonormal sets of basis functions for the spaces  $V_N$  and  $Q_N$ , respectively. In this way, a reduced-order approximation of both velocity and pressure field can be sought under the form

$$\underline{\mathbf{u}}(\boldsymbol{\mu}) \approx Z_{\mathbf{u}} \underline{\mathbf{u}}_N(\boldsymbol{\mu}), \quad \underline{\mathbf{p}}(\boldsymbol{\mu}) \approx Z_p \underline{\mathbf{p}}_N(\boldsymbol{\mu}), \quad (14)$$

where  $\underline{\mathbf{u}}_N(\boldsymbol{\mu}) \in \mathbb{R}^{N_u}$ ,  $\underline{\mathbf{p}}_N(\boldsymbol{\mu}) \in \mathbb{R}^{N_p}$  are determined through a Galerkin projection. To this aim, we impose that the residual obtained by substituting (14) in (8) is orthogonal to the columns of  $Z_{\mathbf{u}}$ ,  $Z_p$ :

$$\begin{bmatrix} Z_{\mathbf{u}}^T & O \\ O & Z_p^T \end{bmatrix} \begin{bmatrix} \underline{\mathbf{f}}(\boldsymbol{\mu}) - (A(\boldsymbol{\mu}) + C(Z_{\mathbf{u}} \underline{\mathbf{u}}_N(\boldsymbol{\mu}); \boldsymbol{\mu})) Z_{\mathbf{u}} \underline{\mathbf{u}}_N(\boldsymbol{\mu}) - B^T(\boldsymbol{\mu}) Z_{\mathbf{u}} \underline{\mathbf{p}}_N(\boldsymbol{\mu}) \\ \underline{\mathbf{g}}(\boldsymbol{\mu}) - B(\boldsymbol{\mu}) Z_{\mathbf{u}} \underline{\mathbf{u}}_N(\boldsymbol{\mu}) \end{bmatrix} = \begin{bmatrix} \mathbf{0} \\ \mathbf{0} \end{bmatrix}.$$

Thus, once we have built the reduced basis for both velocity and pressure fields (during the Offline stage), for any new parameter value  $\boldsymbol{\mu} \in \mathcal{D}$  the following reduced-order problem has to be solved (at the Online stage) to find the NS reduced-order approximation:

$$\begin{bmatrix} A_N(\boldsymbol{\mu}) + C_N(\underline{\mathbf{u}}_N(\boldsymbol{\mu}); \boldsymbol{\mu}) & B_N^T(\boldsymbol{\mu}) \\ B_N(\boldsymbol{\mu}) & 0 \end{bmatrix} \begin{bmatrix} \underline{\mathbf{u}}_N(\boldsymbol{\mu}) \\ \underline{\mathbf{p}}_N(\boldsymbol{\mu}) \end{bmatrix} = \begin{bmatrix} \underline{\mathbf{f}}_N(\boldsymbol{\mu}) \\ \underline{\mathbf{g}}_N(\boldsymbol{\mu}) \end{bmatrix} \quad (15)$$

where, similarly to what shown in [18], [37, Chapter 19],

$$A_N(\boldsymbol{\mu}) = Z_{\mathbf{u}}^T A(\boldsymbol{\mu}) Z_{\mathbf{u}}, \quad B_N(\boldsymbol{\mu}) = Z_p^T B(\boldsymbol{\mu}) Z_{\mathbf{u}}, \quad C_N(\cdot; \boldsymbol{\mu}) = Z_{\mathbf{u}}^T C(\cdot; \boldsymbol{\mu}) Z_{\mathbf{u}}; \quad (16)$$

in the same way, for the right-hand sides we have

$$\underline{\mathbf{f}}_N(\boldsymbol{\mu}) = Z_{\mathbf{u}}^T \underline{\mathbf{f}}(\boldsymbol{\mu}), \quad \underline{\mathbf{g}}_N(\boldsymbol{\mu}) = Z_p^T \underline{\mathbf{g}}(\boldsymbol{\mu}).$$

We point out that a suitable Offline/Online decomposition is made possible thanks to the assumption of affine parametric dependence [38]. Nevertheless, this features some extra difficulties in order to handle nonlinear terms in an efficient way. Our current approach is to store the third order tensor

$$C_N(\varphi_j; \boldsymbol{\mu}) = Z_{\mathbf{u}}^T C(\varphi_j; \boldsymbol{\mu}) Z_{\mathbf{u}}, \quad \forall j = 1, \dots, N_u$$

in order to compute, at each fixed point iteration, the nonlinear term as

$$C_N(\underline{\mathbf{u}}_N(\boldsymbol{\mu}); \boldsymbol{\mu}) = \sum_{j=1}^{N_u} u_N^{(j)} C_N(\varphi_j; \boldsymbol{\mu})$$

and preserve the Offline/Online decomposition. We remark however that such (dense) third order tensor may entail high storage costs; recent alternative approaches make use of a discrete empirical interpolation method [39] or hyper-reduction techniques, such as *gappy POD* [40], or again compressive tensor approximations [41] to alleviate this problem.

#### 4. STABILITY ANALYSIS AND SUPREMIZERS ENRICHMENT

In this Section we show how to get, from the POD modes, a suitable couple of reduced spaces for velocity and pressure in order to fulfill a (reduced version of the) inf-sup condition. To this goal, we provide a detailed stability analysis of the POD-Galerkin ROM we have previously derived.

**4.1. Conditions for solvability and stability of the full-order approximation.** In view of the analysis of the POD-Galerkin ROM, let us briefly recall the conditions ensuring the full-order problem (8) to be solvable and stable. A deep analysis can be found e.g. in [42, 43], whereas we refer to [18] for further details about the analysis in the parametrized case.

For any  $\boldsymbol{\mu} \in \mathcal{D}$ , at each step  $k = 1, 2, \dots$  of the fixed point iteration we need to solve the linear system obtained from (8) by replacing  $C(\underline{\mathbf{u}}(\boldsymbol{\mu}); \boldsymbol{\mu})$  with  $C(\underline{\mathbf{z}}(\boldsymbol{\mu}); \boldsymbol{\mu})$ , being at each step  $\underline{\mathbf{z}}(\boldsymbol{\mu}) = \underline{\mathbf{u}}^{(k)}(\boldsymbol{\mu})$ . In order to obtain stable approximations, we require that

(1) there exists  $\tilde{\alpha}_h > 0$  such that, for any  $\underline{\mathbf{z}}$

$$\alpha_h(\boldsymbol{\mu}) = \inf_{\underline{\mathbf{u}} \in K} \sup_{\underline{\mathbf{v}} \in K} \frac{\underline{\mathbf{v}}^T (A(\boldsymbol{\mu}) + C(\underline{\mathbf{z}}; \boldsymbol{\mu})) \underline{\mathbf{u}}}{\|\underline{\mathbf{v}}\|_V \|\underline{\mathbf{u}}\|_V} \geq \tilde{\alpha}_h > 0 \quad \forall \boldsymbol{\mu} \in \mathcal{D} \quad (\text{F1})$$

being  $K = K(\boldsymbol{\mu}) = \ker(B(\boldsymbol{\mu})) = \{\underline{\mathbf{v}} \in \mathbb{R}^{N_u^h} : B(\boldsymbol{\mu})\underline{\mathbf{v}} = \underline{\mathbf{0}}\}$  the kernel of  $B(\boldsymbol{\mu})$ ;

(2) there exists  $\tilde{\beta}_h > 0$  such that

$$\beta_h(\boldsymbol{\mu}) = \inf_{\underline{\mathbf{q}} \neq \underline{\mathbf{0}}} \sup_{\underline{\mathbf{v}} \neq \underline{\mathbf{0}}} \frac{\underline{\mathbf{q}}^T B(\boldsymbol{\mu}) \underline{\mathbf{v}}}{\|\underline{\mathbf{v}}\|_V \|\underline{\mathbf{q}}\|_Q} \geq \tilde{\beta}_h > 0 \quad \forall \boldsymbol{\mu} \in \mathcal{D}. \quad (\text{F2})$$

In particular, conditions (F1) and (F2) are sufficient to ensure the solvability of the linear system obtained at each iteration of the fixed-point algorithm. The former is related to the stability of the velocity operator – namely, the coercivity of the diffusion term and the continuity of the linearized term – and it is fulfilled whenever a small data condition is satisfied (see e.g. [43]). Under this condition, we can ensure the unique solvability with respect to the velocity. On the other hand, unique solvability with respect to the pressure is rather problematic (as it already happens for a Stokes problem); it is ensured by the latter condition, which is the discrete (parametrized) version of the well-known *Ladyzhenskaya-Brezzi-Babuška* (LBB) inf-sup condition. To meet this requirement, we need to choose a proper couple of velocity and pressure approximation spaces, such as the Taylor-Hood ( $\mathbb{P}_2-\mathbb{P}_1$ ) finite elements. In particular, condition (F2) implies that  $\dim(\ker(B^T(\boldsymbol{\mu}))) = 0$ , so that no *spurious pressure modes* appear at the numerical level. Moreover, we must have  $N_u^h \geq N_p^h$ ; as we will detail later on, it is mandatory to ensure a similar condition at the reduced-order level, too, and to provide a suitable criterion to check its validity.

To this aim, we can express the stability factor  $\beta_h(\boldsymbol{\mu})$  as the solution of the following generalized eigenvalue problem:

$$\begin{bmatrix} X_{\mathbf{u}} & B^T(\boldsymbol{\mu}) \\ B(\boldsymbol{\mu}) & O \end{bmatrix} \begin{bmatrix} \underline{\mathbf{v}} \\ \underline{\mathbf{q}} \end{bmatrix} = -\lambda(\boldsymbol{\mu}) \begin{bmatrix} O & O \\ O & X_p \end{bmatrix} \begin{bmatrix} \underline{\mathbf{v}} \\ \underline{\mathbf{q}} \end{bmatrix}. \quad (17)$$

In this way, the kernel of  $B(\boldsymbol{\mu})$  can be identified with zero eigenvalues of eigenproblem (17): if  $\lambda(\boldsymbol{\mu}) = 0$ , then  $B(\boldsymbol{\mu})\underline{\mathbf{v}} = \underline{\mathbf{0}}$ , so that the nonzero eigenvalues are associated with velocity vectors  $\underline{\mathbf{v}} \notin \ker(B(\boldsymbol{\mu}))$  (and nonzero pressures). In particular, we find

$$B(\boldsymbol{\mu})X_{\mathbf{u}}^{-1}B(\boldsymbol{\mu})^T \underline{\mathbf{q}} = \lambda(\boldsymbol{\mu})X_p \underline{\mathbf{q}} \quad (18)$$

that is, we end up with a Rayleigh-quotient characterization of the nonzero eigenvalues<sup>2</sup>

$$\lambda(\boldsymbol{\mu}) = \frac{(B(\boldsymbol{\mu})X_{\mathbf{u}}^{-1}B(\boldsymbol{\mu})^T \underline{\mathbf{q}}, \underline{\mathbf{q}})}{(X_p \underline{\mathbf{q}}, \underline{\mathbf{q}})} \Rightarrow \beta_h(\boldsymbol{\mu}) = \sqrt{\lambda_1(\boldsymbol{\mu})}, \quad (19)$$

thus providing an equivalent expression of the stability factor; here  $\lambda_1(\boldsymbol{\mu})$  denotes the minimum eigenvalue solution of (17). In fact,

$$\begin{aligned} \beta_h(\boldsymbol{\mu}) &= \inf_{\underline{\mathbf{q}} \neq \underline{\mathbf{0}}} \sup_{\underline{\mathbf{v}} \neq \underline{\mathbf{0}}} \frac{(\underline{\mathbf{q}}, B(\boldsymbol{\mu})\underline{\mathbf{v}})}{(X_p \underline{\mathbf{q}}, \underline{\mathbf{v}})^{1/2}(X_p \underline{\mathbf{q}}, \underline{\mathbf{q}})^{1/2}} = \inf_{\underline{\mathbf{q}} \neq \underline{\mathbf{0}}} \frac{1}{(X_p \underline{\mathbf{q}}, \underline{\mathbf{q}})^{1/2}} \sup_{\underline{\mathbf{w}} = X_{\mathbf{u}}^{1/2} \underline{\mathbf{v}} \neq \underline{\mathbf{0}}} \frac{(X_{\mathbf{u}}^{-1/2} B^T(\boldsymbol{\mu}) \underline{\mathbf{q}}, \underline{\mathbf{w}})}{(\underline{\mathbf{w}}, \underline{\mathbf{w}})^{1/2}} \\ &= \inf_{\underline{\mathbf{q}} \neq \underline{\mathbf{0}}} \frac{(X_{\mathbf{u}}^{-1/2} B^T(\boldsymbol{\mu}) \underline{\mathbf{q}}, X_{\mathbf{u}}^{-1/2} B^T(\boldsymbol{\mu}) \underline{\mathbf{q}})^{1/2}}{(X_p \underline{\mathbf{q}}, \underline{\mathbf{q}})^{1/2}} = \inf_{\underline{\mathbf{q}} \neq \underline{\mathbf{0}}} \frac{(B(\boldsymbol{\mu})X_{\mathbf{u}}^{-1}B(\boldsymbol{\mu})^T \underline{\mathbf{q}}, \underline{\mathbf{q}})^{1/2}}{(X_p \underline{\mathbf{q}}, \underline{\mathbf{q}})^{1/2}} = \sqrt{\lambda_1(\boldsymbol{\mu})} \end{aligned}$$

since the supremum on the first line is reached when  $\underline{\mathbf{w}} = X_{\mathbf{u}}^{-1/2} B^T(\boldsymbol{\mu}) \underline{\mathbf{q}}$ ; for further details see e.g. [44], Chapter 5. We thus remark that, for any  $\underline{\mathbf{q}} \neq \underline{\mathbf{0}}$ , the corresponding *supremizer*, i.e. the element realizing the supremum in (F2), is given by the solution  $\underline{\mathbf{s}}^\mu = \underline{\mathbf{s}}^\mu(\underline{\mathbf{q}})$  of the following problem:  $(X_{\mathbf{u}})^{1/2} \underline{\mathbf{s}}^\mu(\underline{\mathbf{q}}) = X_{\mathbf{u}}^{-1/2} B^T(\boldsymbol{\mu}) \underline{\mathbf{q}}$ , that is,

$$X_{\mathbf{u}} \underline{\mathbf{s}}^\mu(\underline{\mathbf{q}}) = B^T(\boldsymbol{\mu}) \underline{\mathbf{q}}. \quad (20)$$

---

<sup>2</sup>Equivalently, provided that  $\ker(B^T(\boldsymbol{\mu})) = \underline{\mathbf{0}}$ ,  $B(\boldsymbol{\mu})$  has  $N_p^h$  positive singular values  $0 < \sigma_1(\boldsymbol{\mu}) \leq \sigma_2(\boldsymbol{\mu}) \leq \dots \leq \sigma_{N_p^h}(\boldsymbol{\mu})$ , given by  $\sigma_i(\boldsymbol{\mu}) = \sqrt{\lambda_i(\boldsymbol{\mu})}$ .

In other words, the *supremizer* is the element  $\underline{\mathbf{s}}^\mu(\underline{\mathbf{q}})$  which, given  $q \in Q$ , realizes the inf-sup condition. The following properties, useful in the remainder, hold:

**Proposition 1.** *The solution  $\underline{\mathbf{s}}(\boldsymbol{\mu})$  of problem (20) is such that*

$$\underline{\mathbf{s}}^\mu(\underline{\mathbf{q}}) = \arg \sup_{\underline{\mathbf{v}} \neq \underline{\mathbf{0}}} \frac{(\underline{\mathbf{q}}, B(\boldsymbol{\mu})\underline{\mathbf{v}})}{\|\underline{\mathbf{v}}\|_V}; \quad (21)$$

moreover,

$$\beta_h^2(\boldsymbol{\mu}) = \inf_{\underline{\mathbf{q}} \neq \underline{\mathbf{0}}} \frac{\|\underline{\mathbf{s}}^\mu(\underline{\mathbf{q}})\|_V}{\|\underline{\mathbf{q}}\|_Q}. \quad (22)$$

*Proof.* Property (21) easily follows from (20) and Cauchy-Schwarz inequality, that is,

$$\frac{(B^T(\boldsymbol{\mu})\underline{\mathbf{q}}, \underline{\mathbf{v}})}{\|X_{\mathbf{u}}^{1/2}\underline{\mathbf{v}}\|} = \frac{(X_{\mathbf{u}}\underline{\mathbf{s}}^\mu(\underline{\mathbf{q}}), \underline{\mathbf{v}})}{\|X_{\mathbf{u}}^{1/2}\underline{\mathbf{v}}\|} = \frac{(X_{\mathbf{u}}^{1/2}\underline{\mathbf{s}}^\mu(\underline{\mathbf{q}}), X_{\mathbf{u}}^{1/2}\underline{\mathbf{v}})}{\|X_{\mathbf{u}}^{1/2}\underline{\mathbf{v}}\|} \leq \|X_{\mathbf{u}}^{1/2}\underline{\mathbf{s}}^\mu(\underline{\mathbf{q}})\| = \|\underline{\mathbf{s}}^\mu(\underline{\mathbf{q}})\|_V;$$

on the other hand, property (22) is a straightforward consequence, since

$$\beta_h^2(\boldsymbol{\mu}) = \inf_{\underline{\mathbf{q}} \neq \underline{\mathbf{0}}} \frac{(X_{\mathbf{u}}^{-1/2}B^T(\boldsymbol{\mu})\underline{\mathbf{q}}, X_{\mathbf{u}}^{-1/2}B^T(\boldsymbol{\mu})\underline{\mathbf{q}})}{(X_p\underline{\mathbf{q}}, \underline{\mathbf{q}})} = \inf_{\underline{\mathbf{q}} \neq \underline{\mathbf{0}}} \frac{(X_{\mathbf{u}}^{1/2}\underline{\mathbf{s}}(\boldsymbol{\mu}), X_{\mathbf{u}}^{1/2}\underline{\mathbf{s}}^\mu(\underline{\mathbf{q}}))}{(X_p\underline{\mathbf{q}}, \underline{\mathbf{q}})} = \inf_{\underline{\mathbf{q}} \neq \underline{\mathbf{0}}} \frac{\|\underline{\mathbf{s}}^\mu(\underline{\mathbf{q}})\|_V}{\|\underline{\mathbf{q}}\|_Q}.$$

□

Further details about possible ways to express (and check) the inf-sup condition can be found, e.g., in [43, 42, 45, 46]. We also remark that the introduction of supremizers is in fact equivalent to require the notion of *T-coercivity* on the corresponding bilinear form, as shown in [47, 48]. As we will see in Section 5, supremizer solutions play a key role in ensuring the stability of a POD-Galerkin ROM. By properly enriching the reduced spaces of velocity and pressure snapshots with the *supremizer* functions, i.e. the solutions of problem (20) for any element  $\underline{\mathbf{q}}$  corresponding to a pressure snapshot, the resulting ROM will satisfy an equivalent *inf-sup* condition.

**4.2. Supremizers enrichment of the reduced velocity space.** Even though the velocity basis functions are obtained by an inf-sup stable method, a Galerkin projection over the spaces built as in (15) does not guarantee to handle in a proper way either the correct recovery of the pressure, or the fulfilment of the incompressibility constraint. As we will detail in Section 5, this is related to the requirement of an equivalent inf-sup condition at the reduced-order level.

For this reason, we enrich the velocity space  $V_N$  with properly chosen *supremizer solutions*. By mapping each element of  $Z_p$  (that is, each pressure basis function) to a suitable element realizing the inf-sup condition, and inserting those elements in the velocity space, we shall obtain an enriched velocity space  $\tilde{V}_N$  that coupled to the pressure space  $Q_N$  fulfills the inf-sup condition (see Section 4.3). Thus, for any pressure snapshot  $\underline{\mathbf{p}}(\boldsymbol{\mu}^j) \in S_p$ , we find the corresponding supremizer solution  $\underline{\mathbf{s}}(\underline{\mathbf{p}}(\boldsymbol{\mu}^j))$  by solving problem (20), that is,

$$X_{\mathbf{u}}\underline{\mathbf{s}}^\mu(\underline{\mathbf{p}}(\boldsymbol{\mu}^j)) = B^T(\boldsymbol{\mu})\underline{\mathbf{p}}(\boldsymbol{\mu}^j). \quad (23)$$

Then, we compute a POD basis for the supremizer space by considering the SVD of the matrix  $X_{\mathbf{u}}^{1/2}S_{\mathbf{s}}$ , being  $S_{\mathbf{s}} = [\underline{\mathbf{s}}^\mu(\underline{\mathbf{p}}(\boldsymbol{\mu}^1)) \mid \dots \mid \underline{\mathbf{s}}^\mu(\underline{\mathbf{p}}(\boldsymbol{\mu}^n))]$ ; we denote by

$$Z_{\mathbf{s}} = [\underline{\boldsymbol{\eta}}_1 \mid \dots \mid \underline{\boldsymbol{\eta}}_{N_{\mathbf{s}}}] \in \mathbb{R}^{N_{\mathbf{u}}^h \times N_{\mathbf{s}}}$$

the matrix made by  $N_{\mathbf{s}} < n$  supremizer modes. We end up with a velocity space  $\tilde{V}_N$  of dimension  $N_{\mathbf{u}} + N_{\mathbf{s}}$ , given by the direct sum of velocity and supremizer basis functions, where

$$\underline{\mathbf{v}}_N = (v_N^{(1)}, \dots, v_N^{(N_{\mathbf{u}})}, s_N^{(1)}, \dots, s_N^{(N_{\mathbf{s}})})^T \in \mathbb{R}^{N_{\mathbf{u}}+N_{\mathbf{s}}} \leftrightarrow v_N = \sum_{n=1}^{N_{\mathbf{u}}} v_N^{(n)} \boldsymbol{\varphi}_n + \sum_{m=1}^{N_{\mathbf{s}}} s_N^{(m)} \boldsymbol{\eta}_m \in \tilde{V}_N$$

replaces (11)<sub>1</sub>. From now on, we will omit the superscript  $\sim$  for the enriched velocity space, and still denote it by  $V_N$ . Moreover, let us define by

$$(\underline{\mathbf{v}}_N, \underline{\mathbf{w}}_N)_{V_N} = (X_{\mathbf{u}}^N \underline{\mathbf{v}}_N, \underline{\mathbf{w}}_N), \quad (\underline{\mathbf{p}}_N, \underline{\mathbf{q}}_N)_{Q_N} = (X_p^N \underline{\mathbf{p}}_N, \underline{\mathbf{q}}_N) \quad (24)$$

the inner products in the reduced spaces, where  $X_{\mathbf{u}}^N$  and  $X_p^N$  are the reduced mass matrices for velocity and pressure fields, respectively, defined as

$$X_{\mathbf{u}}^N = \begin{bmatrix} X_{\mathbf{u}}^{N,\mathbf{uu}} & X_{\mathbf{u}}^{N,\mathbf{us}} \\ X_{\mathbf{u}}^{N,\mathbf{su}} & X_{\mathbf{u}}^{N,\mathbf{ss}} \end{bmatrix} = \begin{bmatrix} Z_{\mathbf{u}}^T X_{\mathbf{u}} Z_{\mathbf{u}} & Z_{\mathbf{u}}^T X_{\mathbf{u}} Z_{\mathbf{s}} \\ Z_{\mathbf{s}}^T X_{\mathbf{u}} Z_{\mathbf{u}} & Z_{\mathbf{s}}^T X_{\mathbf{u}} Z_{\mathbf{s}} \end{bmatrix}, \quad X_p^N = Z_p^T X_p Z_p. \quad (25)$$

In particular, owing to the orthonormality of basis functions in  $Z_{\mathbf{u}}$  (see (12)),  $Z_{\mathbf{s}}$  and  $Z_p$  (see (13)),  $X_{\mathbf{u}}^{N,\mathbf{uu}}$ ,  $X_{\mathbf{u}}^{N,\mathbf{ss}}$  and  $X_p^N$  are identity matrices; this property enhances the algebraic stability of the resulting ROM. However, we remark that the extra diagonal blocks  $X_{\mathbf{u}}^{N,\mathbf{us}}$  and  $X_{\mathbf{u}}^{N,\mathbf{su}}$  do not vanish because velocity and supremizers basis functions are not mutually orthogonal.

**4.3. Evaluating the inf-sup stability of the reduced-order approximation.** Following Section 4.1, let us discuss under which conditions the POD-Galerkin ROM (15) is stable. For any  $\boldsymbol{\mu} \in \mathcal{D}$ , at each step  $k = 1, 2, \dots$  of the *Online* fixed point iteration, we need to solve the linear system obtained from (15) by replacing  $C_N(\underline{\mathbf{u}}_N(\boldsymbol{\mu}); \boldsymbol{\mu})$  with  $C_N(\underline{\mathbf{z}}_N(\boldsymbol{\mu}); \boldsymbol{\mu})$ , being at each step  $\underline{\mathbf{z}}_N(\boldsymbol{\mu}) = \underline{\mathbf{u}}_N^{(k)}(\boldsymbol{\mu})$ . In order to obtain stable approximations, we require that

- (1) there exists  $\tilde{\alpha}_N > 0$  such that, for any  $\underline{\mathbf{z}}_N$

$$\alpha_N(\boldsymbol{\mu}) = \inf_{\underline{\mathbf{u}}_N \in K_N} \sup_{\underline{\mathbf{v}}_N \in K_N} \frac{\underline{\mathbf{v}}_N^T (A_N(\boldsymbol{\mu}) + C_N(\underline{\mathbf{z}}_N; \boldsymbol{\mu})) \underline{\mathbf{u}}_N}{\|\underline{\mathbf{v}}_N\|_{V_N} \|\underline{\mathbf{u}}_N\|_{V_N}} \geq \tilde{\alpha}_N > 0 \quad \forall \boldsymbol{\mu} \in \mathcal{D} \quad (\text{R1})$$

being  $K_N = \ker(B_N(\boldsymbol{\mu})) = \{\underline{\mathbf{v}}_N \in \mathbb{R}^{N_u} : B_N(\boldsymbol{\mu}) \underline{\mathbf{v}}_N = \underline{\mathbf{0}}\}$  the kernel of  $B_N(\boldsymbol{\mu})$ ;

- (2) there exists  $\tilde{\beta}_N > 0$  such that

$$\beta_N(\boldsymbol{\mu}) = \inf_{\underline{\mathbf{q}}_N \neq \underline{\mathbf{0}}} \sup_{\underline{\mathbf{v}}_N \neq \underline{\mathbf{0}}} \frac{\underline{\mathbf{q}}_N^T B_N(\boldsymbol{\mu}) \underline{\mathbf{v}}_N}{\|\underline{\mathbf{v}}_N\|_{V_N} \|\underline{\mathbf{q}}_N\|_{Q_N}} \geq \tilde{\beta}_N > 0 \quad \forall \boldsymbol{\mu} \in \mathcal{D}. \quad (\text{R2})$$

Numerical evidence shows that the fulfillment of property (R1) is automatic, once the analogous condition (F1) at the full-order level is satisfied and the basis matrices are full-rank. On the other hand, the pressure stability condition (R2) is much more critical to be fulfilled, and is not implied by the full-order pressure stability (F2). Here comes into play the supremizer enrichment.

First of all, we can express the ROM stability factor  $\beta_N(\boldsymbol{\mu})$  as the solution of the following generalized eigenvalue problem:

$$\begin{bmatrix} X_{\mathbf{u}}^N & B_N(\boldsymbol{\mu})^T \\ B_N(\boldsymbol{\mu}) & O \end{bmatrix} \begin{bmatrix} \underline{\mathbf{v}}_N(\boldsymbol{\mu}) \\ \underline{\mathbf{q}}_N(\boldsymbol{\mu}) \end{bmatrix} = -\lambda(\boldsymbol{\mu}) \begin{bmatrix} O & O \\ O & X_p^N \end{bmatrix} \begin{bmatrix} \underline{\mathbf{v}}_N(\boldsymbol{\mu}) \\ \underline{\mathbf{q}}_N(\boldsymbol{\mu}) \end{bmatrix} \quad (26)$$

or, in a similar way,

$$B_N(\boldsymbol{\mu})(X_{\mathbf{u}}^N)^{-1} B_N(\boldsymbol{\mu})^T \underline{\mathbf{q}}_N(\boldsymbol{\mu}) = \lambda(\boldsymbol{\mu}) X_p^N \underline{\mathbf{q}}_N(\boldsymbol{\mu}). \quad (27)$$

Problems (26) and (27) are the reduced-order equivalent of problems (17) and (18) introduced at the full-order level, respectively. In particular, it can be shown that the eigenvalues of problems (26)-(27) are real and non-negative [49]. Denoting by  $\lambda_N^k(\boldsymbol{\mu}) > 0$  the first non-null eigenvalue, if  $k = 1$  the reduced-order model is inf-sup stable and  $\beta_N(\boldsymbol{\mu}) = \sqrt{\lambda_N^1(\boldsymbol{\mu})}$ , otherwise the reduced-order model is not inf-sup stable and  $\beta_N(\boldsymbol{\mu}) = 0$ . In particular, enriching the velocity space with the supremizer solutions ensures the fulfillment of the inf-sup condition (R2), thank to the following

**Proposition 2.** *Assume that the full-order model satisfies the inf-sup stability condition (F2). Then, the POD-Galerkin ROM (15) with supremizer enrichment of the velocity space is inf-sup stable, that is*

$$\beta_N(\boldsymbol{\mu}) \geq \beta_h(\boldsymbol{\mu}) > 0 \quad \forall \boldsymbol{\mu} \in \mathcal{D}. \quad (28)$$

*Proof.* The following inequalities hold:

$$\begin{aligned}\beta_h(\boldsymbol{\mu}) &= \inf_{\underline{\mathbf{q}} \neq \mathbf{0}} \sup_{\underline{\mathbf{v}} \neq \mathbf{0}} \frac{(\underline{\mathbf{q}}, B(\boldsymbol{\mu})\underline{\mathbf{v}})}{\|\underline{\mathbf{v}}\|_V \|\underline{\mathbf{q}}\|_Q} \stackrel{(i)}{\leq} \inf_{\underline{\mathbf{q}}_N \neq \mathbf{0}} \sup_{\underline{\mathbf{v}} \neq \mathbf{0}} \frac{(Z_p\underline{\mathbf{q}}_N, B(\boldsymbol{\mu})\underline{\mathbf{v}})}{\|\underline{\mathbf{v}}\|_V \|Z_P\underline{\mathbf{q}}_N\|_Q} \stackrel{(ii)}{\leq} \inf_{\underline{\mathbf{q}}_N \neq \mathbf{0}} \frac{(Z_p\underline{\mathbf{q}}_N, B(\boldsymbol{\mu})\mathbf{s}^\mu(Z_p\underline{\mathbf{q}}_N))}{\|\mathbf{s}^\mu(Z_p\underline{\mathbf{q}}_N)\|_V \|Z_P\underline{\mathbf{q}}_N\|_Q} \\ &\stackrel{(iii)}{\leq} \inf_{\underline{\mathbf{q}}_N \neq \mathbf{0}} \sup_{\underline{\mathbf{v}}_N \neq \mathbf{0}} \frac{(B^T(\boldsymbol{\mu})Z_p\underline{\mathbf{q}}_N, Z_u\underline{\mathbf{v}}_N)}{\|Z_u\underline{\mathbf{v}}_N\|_V \|Z_P\underline{\mathbf{q}}_N\|_Q} \stackrel{(iv)}{=} \inf_{\underline{\mathbf{q}}_N \neq \mathbf{0}} \sup_{\underline{\mathbf{v}}_N \neq \mathbf{0}} \frac{(\underline{\mathbf{q}}_N, B_N(\boldsymbol{\mu})\underline{\mathbf{v}}_N)}{\|\underline{\mathbf{v}}_N\|_{V_N} \|\underline{\mathbf{q}}_N\|_{Q_N}} = \beta_N(\boldsymbol{\mu})\end{aligned}$$

where we have exploited the following facts: (i)  $Q_N \subset Q_h$ ; (ii) the supremizer's definition (23); (iii) the enrichment of the velocity space by supremizers solutions; (iv) the relation  $Z_u^T B^T(\boldsymbol{\mu}) Z_p = B_N^T(\boldsymbol{\mu})$  and the definition of reduced norms, that is

$$\|Z_p\underline{\mathbf{q}}_N\|_Q^2 = (X_p Z_p \underline{\mathbf{q}}_N, Z_p \underline{\mathbf{q}}_N) = (Z_p^T X_p Z_p \underline{\mathbf{q}}_N, \underline{\mathbf{q}}_N) = (X_p^N \underline{\mathbf{q}}_N, \underline{\mathbf{q}}_N) = \|\underline{\mathbf{q}}_N\|_{Q_N}^2$$

thanks to (24)-(25); a similar relation holds for the velocity norms.  $\square$

The addition of the supremizers to the velocity space has been inspired by the greedy-RB setting; see e.g. [28, 29, 27] and different approaches therein. However:

- condition (28) might be in some cases too restrictive, that is, we could have  $\beta_N(\boldsymbol{\mu}) > 0$  without necessarily require that  $\beta_N(\boldsymbol{\mu}) \geq \beta_h(\boldsymbol{\mu})$ ;
- the evaluation of the *exact* supremizers  $s^\mu(\cdot)$  would lead to a  $\boldsymbol{\mu}$ -dependent velocity space, because of the dependence on  $B^T(\boldsymbol{\mu})$  in (23), and thus deteriorates the offline/online efficiency. Hence, we rather consider some *approximate* supremizers, that is, we solve (23) by considering (offline) the same  $\boldsymbol{\mu} = \boldsymbol{\mu}^j$  values used to store velocity and pressure solutions, and an enriched (online) velocity space obtained by adding  $N_s$  supremizer POD modes.

If we rely on *approximate* supremizers we cannot rigorously demonstrate (28); however, we can provide some heuristic criteria to ensure that  $\beta_N(\boldsymbol{\mu}) > 0$  (yielding therefore stability): this is the goal of the following section.

Before proceeding further, let us mention that other stabilization approaches are also possible, but would require much care in case of geometrical variation. We refer to [26, 21] for an online stabilization with a streamline-upwind/Petrov-Galerkin (SUPG) and pressure-stabilizing/Petrov-Galerkin (PSPG) method. When dealing with fixed geometries, a pressure-Poisson approach for the recovery of the pressure can be considered as a particular case of the SUPG/PSPG stabilization (see e.g. [24]). Further details about other possible approaches can be found, for instance, in [8, 7]. Our belief – confirmed by the analysis reported in the following sections – is that the supremizer enrichment yields a very competitive alternative to the strategies mentioned above, for what is concerned with online computational costs. In fact, although our method requires larger online data structures (because of the additional  $N_s$  basis functions), no additional assembly and storage of terms related to SUPG/PSPG stabilization is needed.

## 5. HEURISTIC CRITERIA FOR ONLINE SUPREMIZERS ENRICHMENT

In this section we give further insights on the stability of the POD-Galerkin ROM, and by providing some practical criteria for the online supremizers enrichment.

The aim of this section and of the numerical results in the next section is to provide answers and numerical evidence to the following questions:

- Q1. for which values of  $(N_u, N_s, N_p)$  is the online system stable?
- Q2. which values of  $(N_u, N_s, N_p)$  prevent an online locking phenomenon to occur?
- Q3. for which values of  $(N_u, N_s, N_p)$  the reduced-order model satisfies an inf-sup condition, provided that the same condition is satisfied at the full-order level?

As shown in Section 3, a computation of the inf-sup constant can be carried out in order to check the online stability of the reduced-order model. Question Q1 is thus related to the dimension of  $\ker(B_N(\boldsymbol{\mu})^T)$ , that is, to the possible occurrence of spurious pressure modes for

the reduced-order model. As of question Q2, locking phenomena occur if  $\beta_N(\boldsymbol{\mu}) \rightarrow 0$  as  $N$  “increases”. Finally, question Q3 is equivalent to check whether the inequality  $\beta_N(\boldsymbol{\mu}) \geq \beta_h(\boldsymbol{\mu})$  holds.

An a priori practical criterion for online supremizers enrichment will be detailed in this section and is inspired by question Q1. Questions Q2 and Q3 will be answered in the next section, by means of some numerical test cases.

**5.1. Case I: physical parametrization only.** In the case of parametrized problems involving only physical parameters, a criterion for the selection of the number  $N_s$  of supremizer is to assume  $N_s \geq N_p$ . As a matter of fact, let us consider the matrix

$$B_N(\boldsymbol{\mu})^T = \begin{bmatrix} B_{N,p\mathbf{u}}(\boldsymbol{\mu})^T \\ B_{N,p\mathbf{s}}(\boldsymbol{\mu})^T \end{bmatrix} \in \mathbb{R}^{(N_u+N_s) \times N_p}$$

where  $B_{N,p\mathbf{s}}(\boldsymbol{\mu})^T \in \mathbb{R}^{N_s \times N_p}$ ,  $B_{N,p\mathbf{u}}(\boldsymbol{\mu})^T \in \mathbb{R}^{N_u \times N_p}$ . The block  $B_{N,p\mathbf{u}}(\boldsymbol{\mu})^T$  is identically zero because each velocity basis function is divergence free. Then, a necessary condition for  $B_N(\boldsymbol{\mu})^T$  to be full-rank is that  $N_s \geq N_p$ . More insights on the practical convenience entailed by choosing  $N_s = N_p$  or  $N_s > N_p$  will be given in the next section.

**5.2. Case II: physical and geometrical parametrization.** In the case of both physical and a geometrical parameters, a possible criterion for the online supremizers enrichment is based on the following result:

**Proposition 3.** *Let  $\lambda_N^k(\boldsymbol{\mu}) > 0$ ,  $k = k(N_u, N_s, N_p; \boldsymbol{\mu}) \in \mathbb{N}$ , be the first non-null eigenvalue of the generalized eigenvalue problem (26). The following relation holds:*

$$k_{pm} = k - 1 + N_p - N_u - N_s > 0 \implies \dim(\ker B_N(\boldsymbol{\mu})^T) > 0.$$

*Proof.* Equivalently, we shall prove the following:

$$\dim(\ker B_N(\boldsymbol{\mu})^T) = 0 \implies k_{pm} = k - 1 + N_p - N_u - N_s \leq 0.$$

For the sake of brevity the dependence on  $\boldsymbol{\mu}$  is omitted. Let

$$M_N = \begin{bmatrix} X_u^N & B_N^T \\ B_N & O \end{bmatrix}, \quad S_N = B_N (X_u^N)^{-1} B_N^T.$$

(1) From (26), it follows that  $\dim(\ker M_N) = k - 1$ . Moreover, from the Guttman rank additivity formula

$$\text{rank } M_N = \text{rank } X_u^N + \text{rank } S_N,$$

it follows that

$$\dim(\ker S_N) = N_p - \text{rank } M_N + \text{rank } X_u^N = k - 1.$$

(2) Furthermore, we have

$$\dim(\ker B_N^T) = N_p - \text{rank } B_N^T = N_p - \text{rank } B_N = N_p - N_u - N_s + \dim(\ker B_N).$$

(3) Finally, owing to the hypothesis  $\dim(\ker B_N(\boldsymbol{\mu})^T) = 0$  and the invertibility of  $X_u^N$ ,

$$\begin{aligned} k - 1 &= \dim(\ker S_N) = \dim[((X_u^N)^{-1} B_N^T)^{-1} (\ker B_N)] \leq \\ &\leq \dim[(\ker((X_u^N)^{-1} B_N^T))] + \dim(\ker B_N) = N_u + N_s - N_p. \end{aligned}$$

□

The previous proposition is an extension to the ROM framework of a similar result holding for the full-order model [46]. We will rely on this criterion in the next section to detect the existence of spurious pressure modes; as we will see, in practice, this criterion is able to discard the choices  $N_s = 0$ . More insights on questions Q2 and Q3 will also be provided in the next section.

## 6. NUMERICAL RESULTS: BACKWARD FACING STEP FLOW

In this section we show some numerical results obtained by means of our POD-Galerkin ROM in the case of a two-dimensional backward facing step flow (see the geometry shown in Figure 1). Moreover, we provide both an inf-sup stability analysis and an error analysis, confirming the results described in Section 5.

In particular, we consider two different test cases, dealing with (I) physical parameters only and (II) both physical and geometrical parameters, given as follows:

- *Physical parameters.* The viscosity  $\nu$  and the horizontal inlet velocity  $u_{\text{in}}$  are considered as physical parameters  $\boldsymbol{\mu}_p = (\nu, u_{\text{in}})$ . The resulting range of Reynolds number is [0.75, 300] (based on the inlet velocity and the inlet height  $h$ ).
- *Geometrical parameters.* The step height  $H_o$  is the geometrical parameter  $\boldsymbol{\mu}_g = (H_o)$ , chosen so that the ratio  $H_o/H$  varies in [0.5, 1.5]. In order to map the reference domain  $\bar{\Omega} = \bar{\Omega}_1 \cup \bar{\Omega}_2$  onto the deformed configuration  $\bar{\Omega}(\boldsymbol{\mu}_g) = \bar{\Omega}_1 \cup \bar{\Omega}_2(\boldsymbol{\mu}_g)$  we consider the transformation  $\mathbf{x}_o = \mathbf{T}(\mathbf{x}; \boldsymbol{\mu}_g)$  defined as

$$\begin{cases} x_{1,o} &= x_1 \\ x_{2,o} &= \begin{cases} x_2, & x_2 \geq -h, \\ -h + \frac{H_o}{H}(x_2 + h), & x_2 < -h. \end{cases} \end{cases}$$

In this way, an immediate offline-online decomposition of the parametrized tensors in (5) is recovered, since the map  $\mathbf{T}(\cdot; \boldsymbol{\mu}_g)$  is affine.

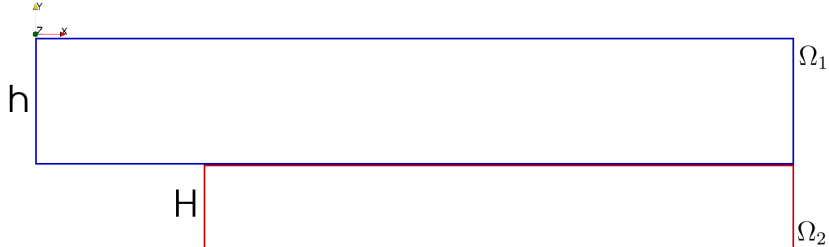


FIGURE 1. Domain: a two-dimensional backward facing step.

*Computational details of the offline stage.* The offline stage is performed over a random set of  $N_{\text{train}} = 300$  snapshots, solving for each snapshot the parametrized Navier-Stokes problem and the corresponding supremizer problem. A Taylor-Hood  $\mathbb{P}_2 - \mathbb{P}_1$  FE discretization with 116,136 degrees of freedom has been considered; moreover, to ensure a good sampling over higher Reynolds numbers, a logarithmic scaling on  $\nu$  and  $u_{\text{in}}$  has been performed. Computational details of the offline stage are summarized in Table 1; this stage is performed in parallel on an Intel Westmere 2.40 GHz cluster.

*POD singular values and basis functions.* The decay of POD singular values is shown in Figure 2(a) in the case of physical parameters only, and in Figure 2(b) for the case of both physical and geometrical parameters. As we could expect, considering an additional geometrical parameter implies a slower decay of the singular values w.r.t. the case of Figure 2(a). The first basis functions for velocity, supremizers and pressure are given by the first POD modes (with an additional function used to store the lifting) and are shown in Figure 3. With the exception of the first POD mode, the geometrical variation significantly affects the qualitative behavior of the POD modes.

*Online results.* Some representative ROM solutions for different Reynolds number and step heights are shown in Figure 4; corresponding errors between truth and reduced solutions are reported in Figure 5. We can observe that our ROM is able to correctly capture the flow variability with respect to both physical and geometrical features. The online (nonlinear) ROM

Case	Case I	Case II
Physical parameters	2: $\nu, u_{\text{in}}$	2: $\nu, u_{\text{in}}$
Range $\nu$	[0.05, 2]	[0.05, 2]
Range $u_{\text{in}}$	[0.5, 5]	[0.5, 5]
Resulting range of Reynolds number	[0.75, 300]	[0.75, 300]
Geometrical parameters	0	1: $H_o$
Range $H_o/H$	—	[0.5, 1.5]
$N_{\text{train}}$	300	300
POD offline CPU time	3 h $\times$ 6 processors	5 h $\times$ 6 processors
$N_{\text{max}}$	100	100

TABLE 1. Computational details of the offline stage.

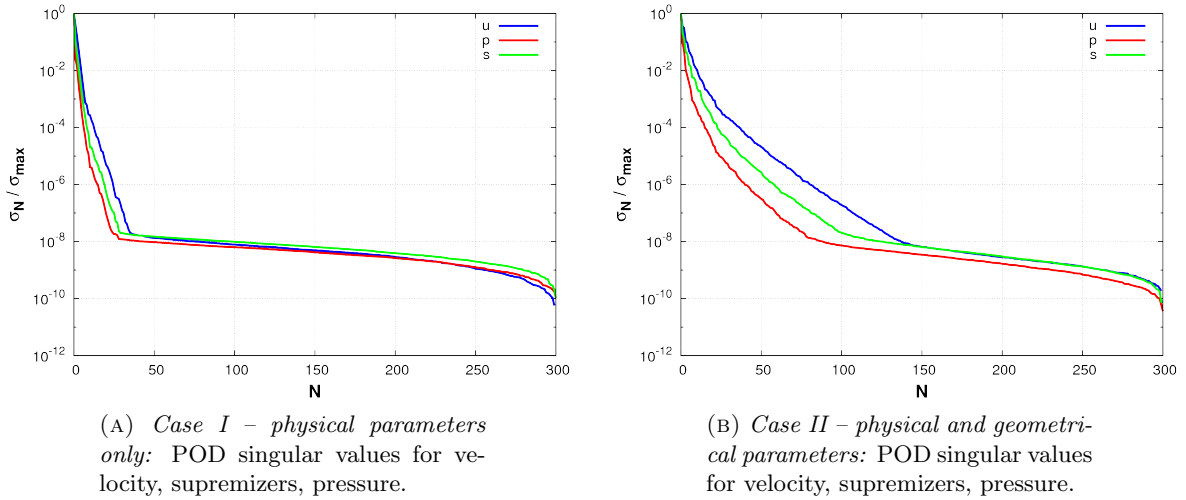


FIGURE 2. Results of the offline stage: POD singular values for velocity, supremizers, pressure.

takes about 5 seconds to run, in serial, on a laptop, thus leading to a speedup of more than one order of magnitude in CPU times, for each online query.

**6.1. Analysis of the ROM – case I (physical parameters only).** In this section an analysis of the ROM is performed for the case of physical parametrization. Figures 6 and 7 report stability factors and relative errors for some representative values of the Reynolds number and different choices  $N_s$  and  $N_u = N_p$ . These results provide a useful insight, showing that, in the case of physical parameters only, it is sufficient to consider  $N_s \geq N_p$  supremizers to obtain both a stable reduced-order model and to ensure that  $\beta_N(\mu) \geq \beta(\mu)$ . Thus, in this case, the three questions Q1, Q2, Q3 lead to the same conclusion. We underline again that the supremizer are subject to a POD procedure too: with respect to the most expensive *exact* supremizer options with online parametric dependence, the less expensive *approximate* option is successfully exploited.

We also remark that, although necessary to obtain a stable system, ROM solution components corresponding to supremizer basis functions are actually smaller than the smallest component related to (divergence-free) velocity basis functions. Thanks to the rapid decay of the singular values a choice  $N_u, N_s, N_p \approx 20$  is sufficient to obtain an accurate reduced-order solution.

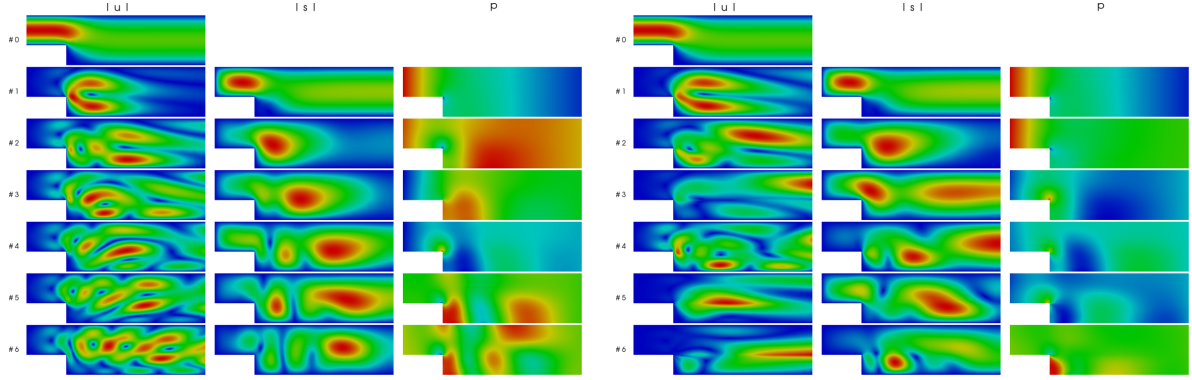
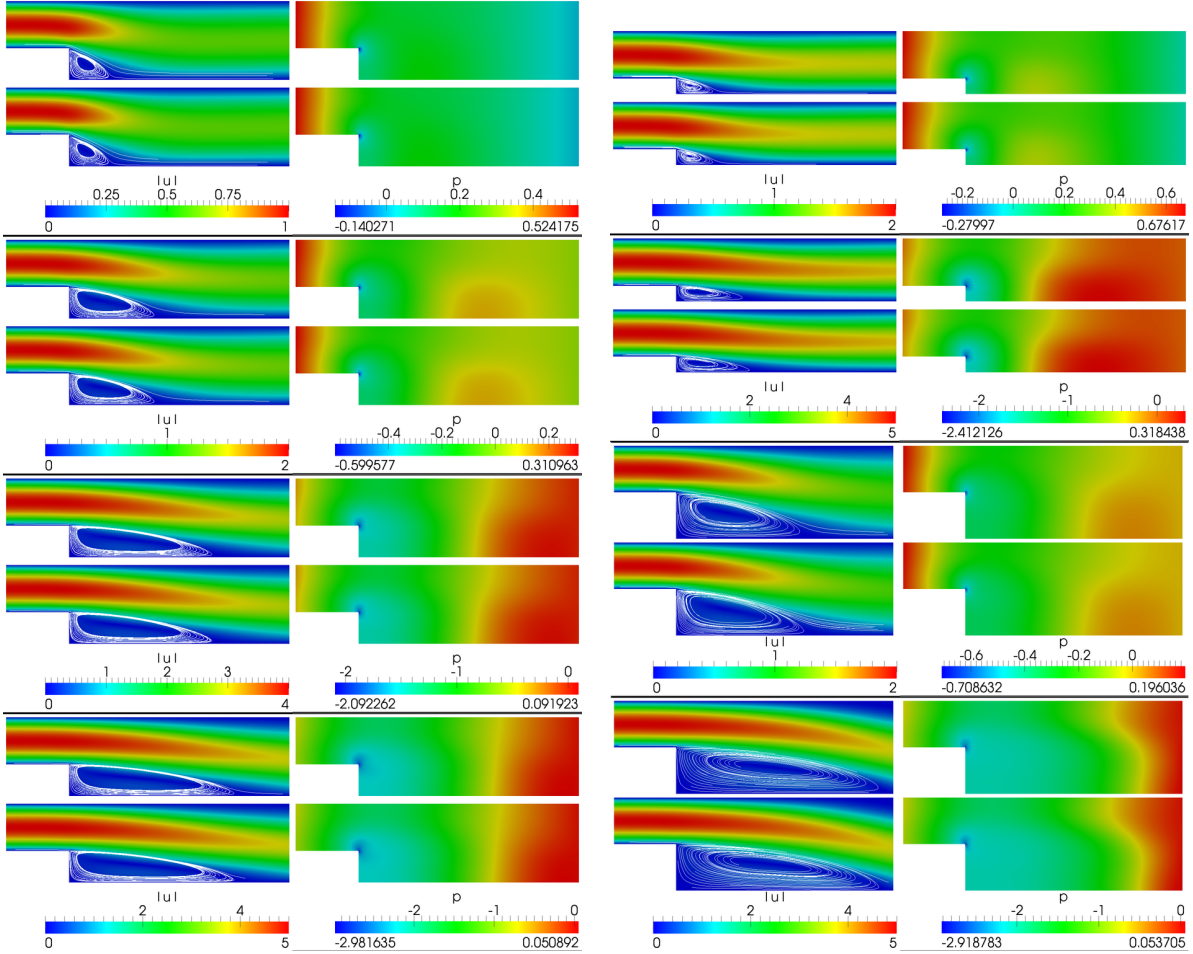


FIGURE 3. Results of the offline stage: first basis functions for velocity, supremizers, pressure.

**6.2. Analysis of the ROM – case II (physical and geometrical parameters).** We now turn to the second case, dealing with both physical and geometrical parameters. Compared to the former, this case requires a more detailed analysis. Figures 8 and 9 show a plot of the stability factors  $\beta_N(\boldsymbol{\mu})$  and of the relative errors for representative values of the parameters and for different choices  $N_s$  and  $N_u = N_p$ . Moreover, we report in Table 2 the evaluation of the quantities introduced in Proposition 3 (namely, the computed values of  $k = k(N_u, N_s, N_p; \boldsymbol{\mu})$  and  $k_{pm} = k_{pm}(N_u, N_s, N_p; \boldsymbol{\mu})$ , together with the value of  $\beta_N(\boldsymbol{\mu})$  and the norm of the reduced pressure  $\|\underline{\mathbf{p}}_N\|_{Q_N}$ ), for increasing values of  $N_s$  and  $N_u = N_p = 30$ . We consider  $Re = 150$  and  $H_o/H = 1$ , indeed similar results can be obtained on the whole parameters range.

Thanks to these results, we can answer the questions highlighted in Section 5 as follows:

- Q1. In order to ensure  $\dim(\ker B_N(\boldsymbol{\mu})^T) = 0$ , it is necessary to enrich the velocity space by adding at least a few supremizers. In fact, when  $N_s = 0$  or  $N_s = 1$ , Table 2 (first and second rows, respectively) shows that  $k_{pm} > 0$ . Then, from Proposition 3, it follows that spurious pressure modes occur. Numerically, this is confirmed by the large value of  $\|\underline{\mathbf{p}}_N\|_{Q_N}$  (see also Figure 10, first and second rows). Moreover, an incorrect approximation of the velocity would be provided by the ROM in these cases (see Figure 10, first row, image on the left).
- Q2. An online locking phenomenon ( $\beta_N(\boldsymbol{\mu}) \rightarrow 0$ ) may occur if too few supremizers are considered, say  $0 < N_s < N_p/2$  (see Figure 8). Table 2 (rows 3 and 4) shows that for  $N_s = 5$  or  $N_s = 7$ , even though the ROM is inf-sup stable and the velocity is correctly approximated, yet the pressure is not recovered accurately (see also Figure 10, rows 3 and 4). However, if enough supremizers are considered (say,  $N_s > N_p/2$ ) the ROM is not only inf-sup stable but allows also to get a better a qualitative agreement with the truth FE solutions. The correct order of magnitude for the solution is recovered (see Table 2, rows 5 and 6,  $N_s = 10, 15$ , respectively, and Figure 10, rows 5 and 6). Moreover, stability factors increase (and errors decrease) as long as  $N_s$  increases (see Figure 9).
- Q3. As in the case of the previous subsection, we obtain that  $\beta_N(\boldsymbol{\mu}) \geq \beta(\boldsymbol{\mu})$  if  $N_s \geq N_p$  (see Figure 8). Thus, choosing  $N_s$  equal to  $N_p$  guarantees the ROM stability, provided that the full-order model is stable. Moreover,  $N_s$  should not be taken strictly greater than  $N_p = N_u$  because (i) the online system dimension would increase and (ii) the algebraic stability of the system deteriorates, so that more iterations of the nonlinear solver would



(A) *Case I – physical parameters only:* velocity and pressure. From top to bottom:  $Re = 30$ ,  $Re = 85$ ,  $Re = 170$ ,  $Re = 215$ .

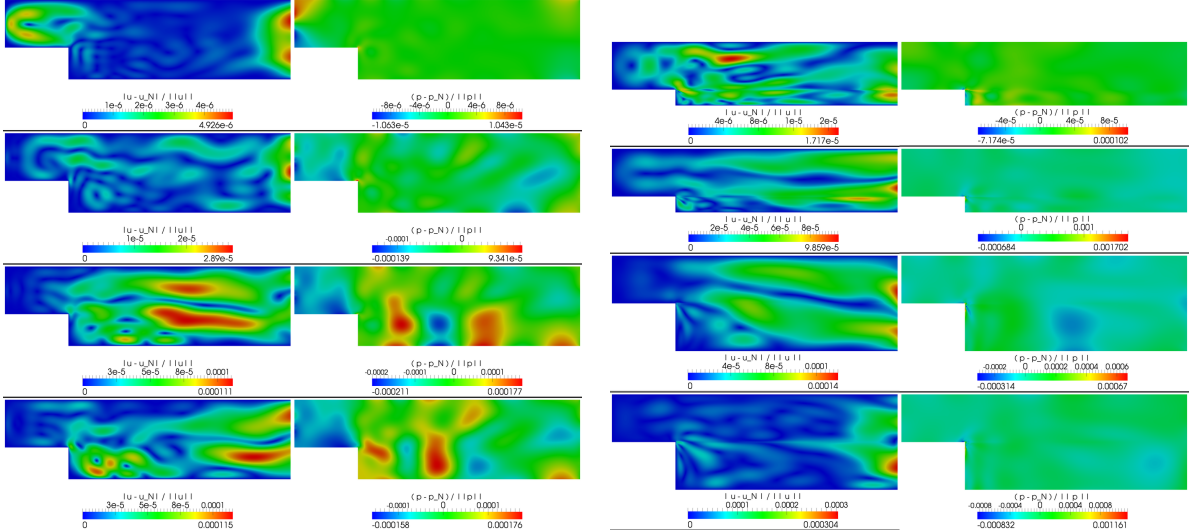
(B) *Case II – physical and geometrical parameters:* velocity and pressure. From top to bottom: ( $Re = 85$ ,  $H_o/H = 0.5$ ), ( $Re = 215$ ,  $H_o/H = 0.5$ ), ( $Re = 85$ ,  $H_o/H = 1.5$ ), ( $Re = 215$ ,  $H_o/H = 1.5$ ).

FIGURE 4. Some representative cases of flow over a backward facing step, with a comparison between truth and reduced-order solutions. Reduced-order solutions were obtained for  $N_u = N_p = N_s = 50$ .

be needed to converge. The latter drawback is due to the fact that the supremizers and velocities basis functions are orthonormal separately into two different sets.

## 7. CONCLUSIONS

In this work a POD-Galerkin reduced basis method, with space construction carried out by proper orthogonal decomposition for velocity and pressure, has been proposed to approximate steady nonlinear parametrized viscous flows at different flow regimes (Reynolds number varying between 1 and 300) and in different domains, properly parametrized. An enrichment procedure of the velocity space by supremizer solutions has been exploited in this context to ensure the stability and the fulfillment of a inf-sup stability condition at the reduced order level. This procedure, adapted from reduced basis methods, can be efficiently employed in this context by performing offline a proper orthogonal decomposition not only on the velocity and pressure snapshots, but also on the set of (approximate) supremizers solutions. In this way, we still



(A) *Case I – physical parameters only:* relative errors for velocity and pressure. From top to bottom:  $Re = 30, Re = 85, Re = 170, Re = 215$ .

(B) *Case II – physical and geometrical parameters:* relative errors for velocity and pressure. From top to bottom:  $(Re = 85, H_o/H = 0.5)$ ,  $(Re = 215, H_o/H = 0.5)$ ,  $(Re = 85, H_o/H = 1.5)$ ,  $(Re = 215, H_o/H = 1.5)$ .

FIGURE 5. Relative errors between truth and reduced-order solutions for some representative cases of flow over a backward facing step. Reduced-order solutions were obtained for  $N_u = N_p = N_s = 50$ .

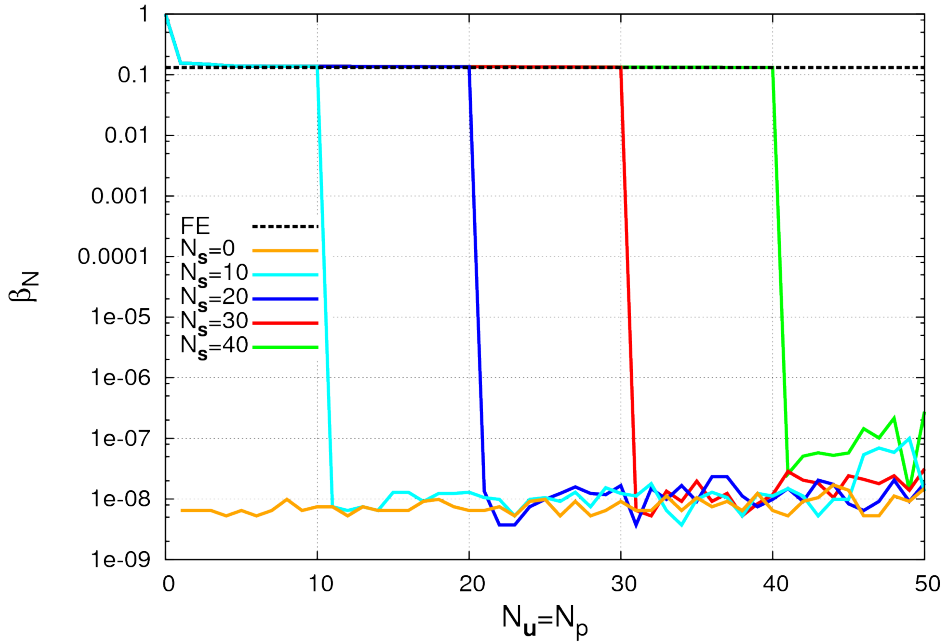


FIGURE 6. *Case I – physical parameters only:* analysis of the stability factor  $\beta_N(\mu)$ .

preserve the stabilization properties, but at a greatly reduced cost, thanks to an efficient offline-online computational decoupling. In fact, this latter would be much more difficult to obtain if we had considered an exact supremizers approach. Heuristic criteria for an online enrichment

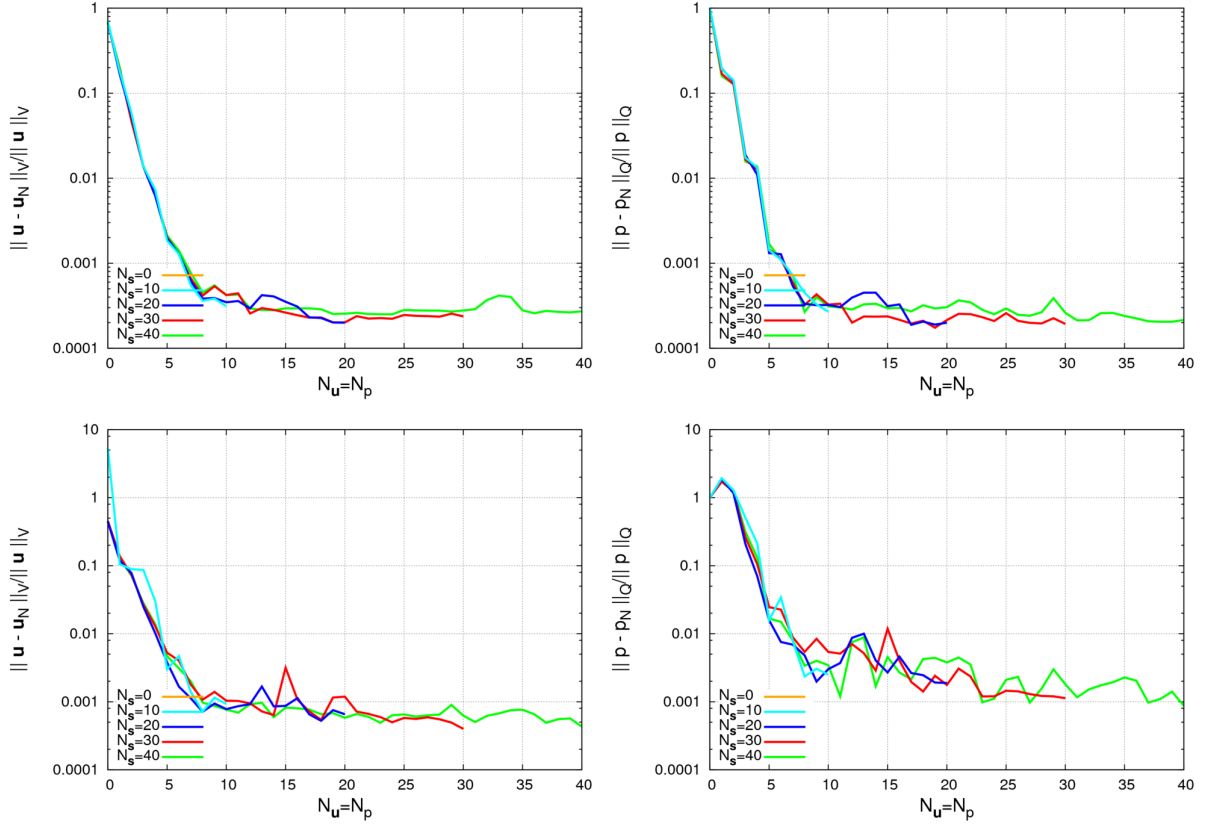


FIGURE 7. *Case I – physical parameters only:* error analysis on velocity (left) and pressure (right) components. Top:  $Re = 30$ ; bottom  $Re = 90$ , respectively. Error analysis is not performed for  $N_s < N_p$  because in these cases reduced system would be singular.

$N_s$	$k$	$k_{pm}$	spurious pressure modes	$\beta_N(\mu)^2$	$\ \underline{\mathbf{p}}_N\ _2$
0	5	4	yes	< tol	1.1653e+09
1	4	2	yes	< tol	7.5223e+06
5	1	-5	no	1.8201e-09	4.3631e+02
7	1	-7	no	3.3185e-08	2.6174e+01
10	1	-10	no	1.0258e-06	1.1228e+01
15	1	-15	no	1.6581e-05	1.1078e+01
30	1	-30	no	1.7305e-02	1.1061e+01
FOM	—	—	no	1.7312e-02	—

TABLE 2. *Case II – physical and geometrical parameters:* stability analysis of the reduced problem ( $Re = 150$ ,  $H_o/H = 1$ ,  $N_u = N_p = 30$ ).

have also been discussed, showing both a theoretical result to detect the existence of spurious pressure modes, and numerical examples to relate the number  $N_s$  of supremizers to the choices of  $N_u$  and  $N_p$ . These results show that at least a few supremizers should be added to the reduced velocity space to obtain a stable ROM. Moreover, in the case of physical parametrization only, a good choice suggested by the current analysis is  $N_s = N_p$ , whereas in the case of both physical and geometrical parameters a reliable method can be obtained also for smaller  $N_s$ , say  $N_s > N_p/2$ . The chance to apply the supremizer enrichment also within a POD context, shown in this work, makes POD a viable alternative to greedy RB methods in order to recover pressure fields whenever (i) an accurate and rapid error bound is not available or (ii) lower

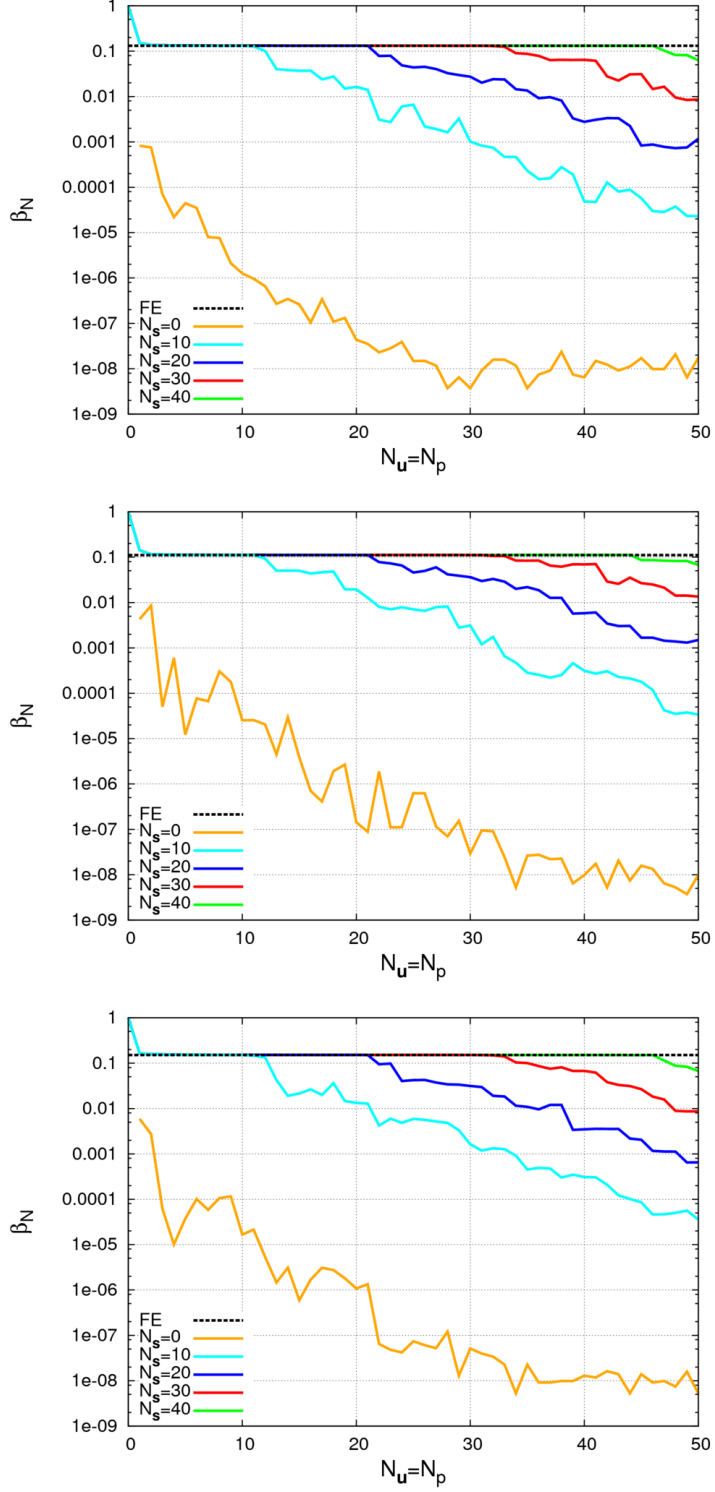


FIGURE 8. *Case II – physical and geometrical parameters:* analysis of the stability factor  $\beta_N(\mu)$ . Top:  $H_o/H = 1$ ; center:  $H_o/H = 0.5$ ; bottom:  $H_o/H = 1.5$ .

bound to parametrized stability factors are not easy to obtain [17, 18, 2]. Further attention will be devoted to time dependent parametrized problems and error bounds calculation, as well as to the case of higher Reynolds number flows.

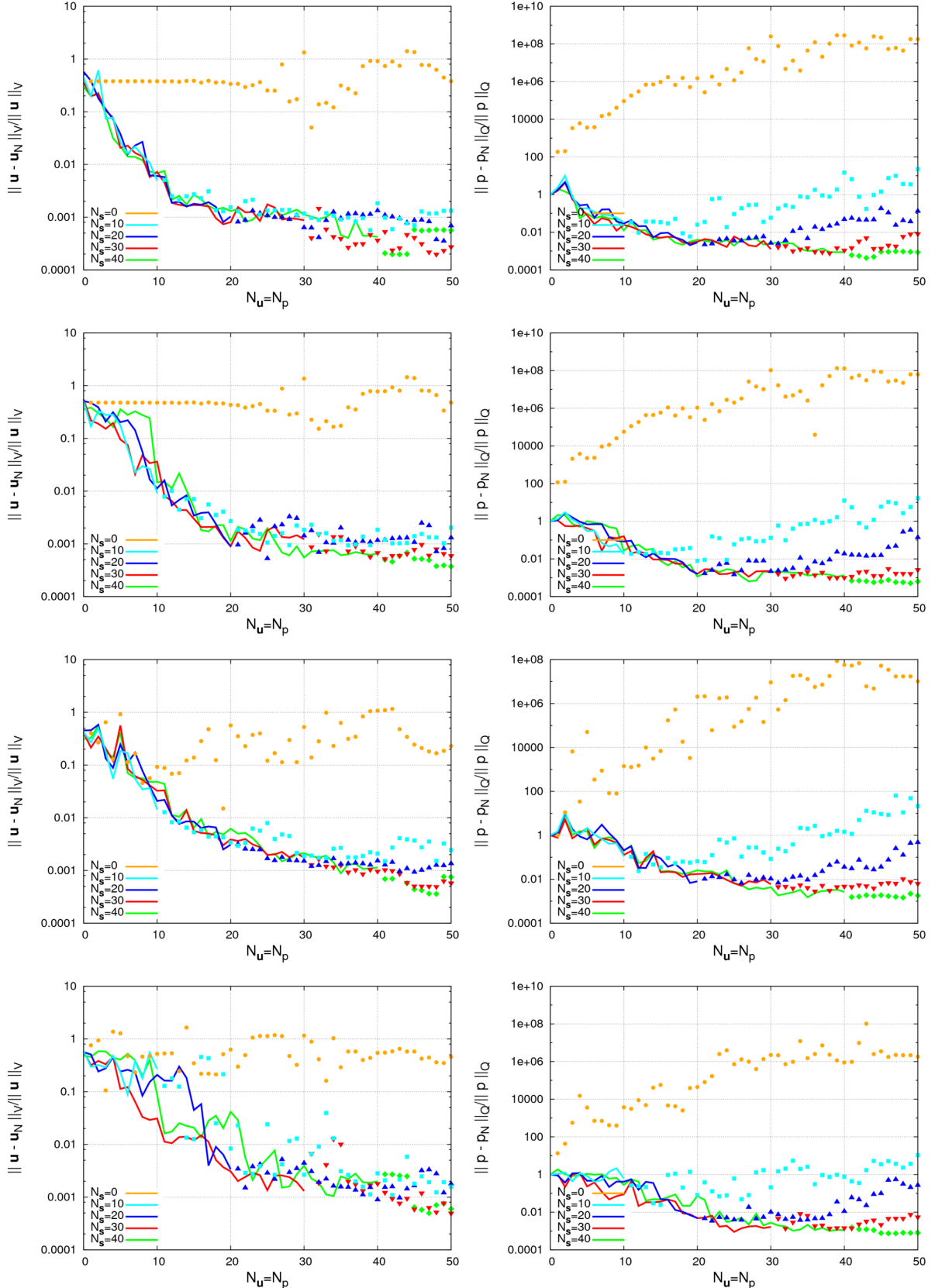


FIGURE 9. *Case II – physical and geometrical parameters:* error analysis on velocity (left) and pressure (right) components. From top to bottom: ( $Re = 90$ ,  $H_o/H = 1$ ), ( $Re = 150$ ,  $H_o/H = 1$ ), ( $Re = 150$ ,  $H_o/H = 0.5$ ), ( $Re = 150$ ,  $H_o/H = 1.5$ ).

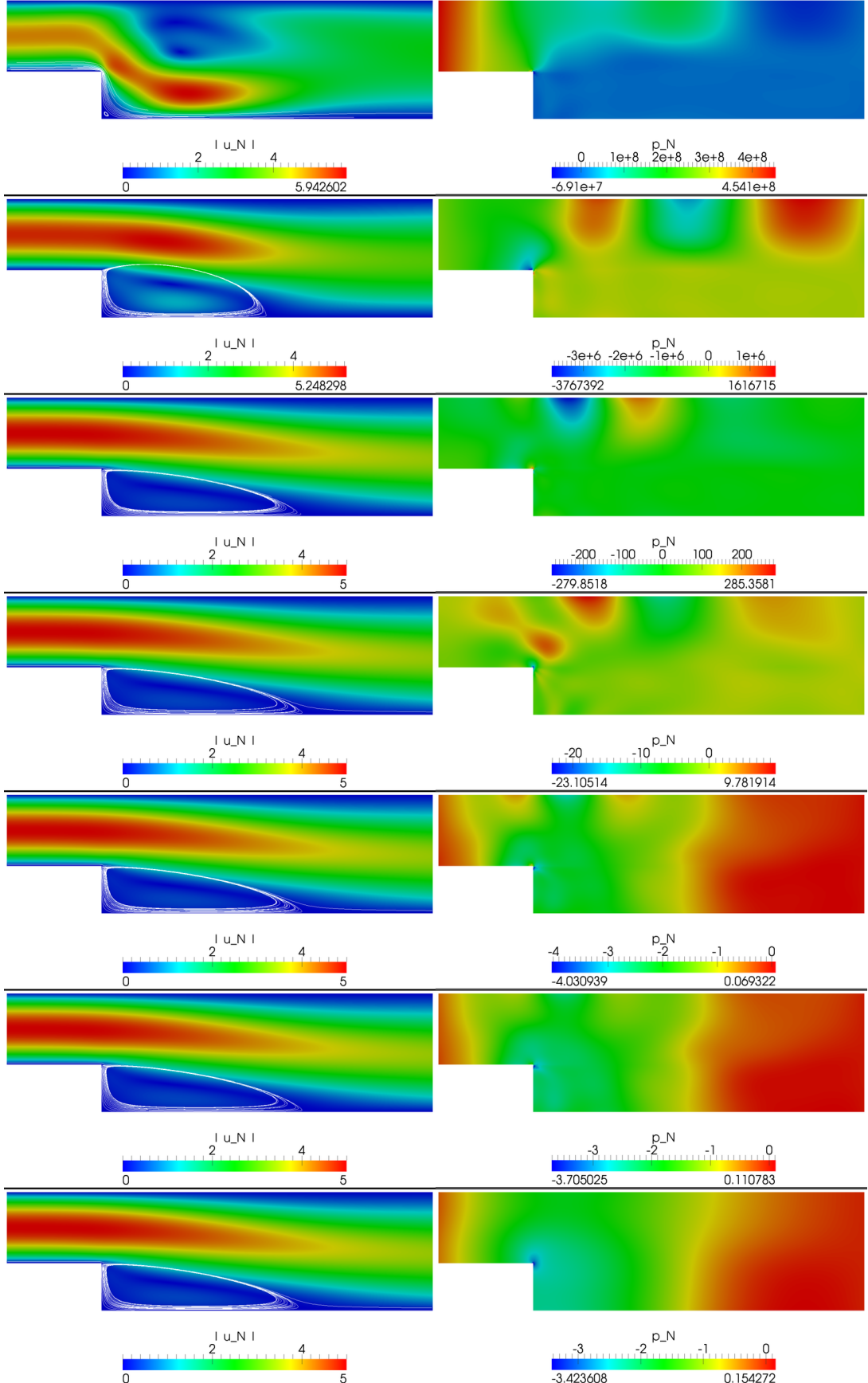


FIGURE 10. *Case II – physical and geometrical parameters:* reduced-order solutions at  $Re = 150$ ,  $H_o/H = 1$ , for  $N_u = N_p = 30$  (left: velocity, right: pressure). From top to bottom:  $N_s = \{0, 1, 5, 7, 10^1, 15, 30\}$ .

## ACKNOWLEDGEMENTS

We acknowledge the use CINECA supercomputing facilities (PLX) within the project CO.GE.STRa (Computational and Geometrical Reduction Strategies) at SISSA and the use of the library `rb00mit` within `libMesh` [50, 51]. We thank Dr. Marco Compagnoni (Dip. Matematica, Politecnico di Milano) for some helpful discussions. The work of Andrea Manzoni has been supported by the SHARM 2012-2014 SISSA post-doctoral research grant on the project “Reduced Basis Methods for shape optimization in computational fluid dynamics”. Gianluigi Rozza acknowledges the SISSA Excellence Grant NOFYSAS “Computational and Geometrical Reduction Strategies for the simulation, control and optimization of complex systems”.

## REFERENCES

- [1] T. Lassila, A. Manzoni, A. Quarteroni, and G. Rozza, *Model order reduction in fluid dynamics: challenges and perspectives*, Reduced Order Methods for Modeling and Computational Reduction (A. Quarteroni and G. Rozza, eds.), vol. 9, Springer Milano, MS&A Series, 2013, pp. 235–274.
- [2] A. Manzoni and F. Negri, *Rigorous and heuristic strategies for the approximation of stability factors in nonlinear parametrized PDEs*, Technical report MATHICSE 8.2014: <http://mathicse.epfl.ch/>, submitted, 2014.
- [3] N. Aubry, P. Holmes, J. Lumley, and E. Stone, *The dynamics of coherent structures in the wall region of a turbulent boundary layer*, J. Fluid Mech. **192** (1988), no. 115, 173–355.
- [4] W. Cazemier, R.W.C.P. Verstappen, and A.E.P. Veldman, *Proper orthogonal decomposition and low-dimensional models for driven cavity flows*, Phys. Fluids **10** (1998), no. 7, 1685–1699.
- [5] G. Berkooz, P. Holmes, and J.L. Lumley, *The Proper Orthogonal Decomposition in the Analysis of Turbulent Flows*, Annu. Rev. Fluid Mech. **25** (1993), no. 1, 539–575.
- [6] S.S. Ravindran, *A reduced-order approach for optimal control of fluids using proper orthogonal decomposition*, Int. J. Numer. Meth. Fluids **34** (2000), 425–448.
- [7] J. Weller, E. Lombardi, M. Bergmann, and A. Iollo, *Numerical methods for low-order modeling of fluid flows based on POD*, Int. J. Numer. Meth. Fluids **63** (2010), no. 2, 249–268.
- [8] M. Bergmann, C.H. Bruneau, and A. Iollo, *Enablers for robust POD models*, J. Comp. Phys. **228** (2009), no. 2, 516–538.
- [9] A. Iollo, S. Lanteri, and J.A. Désidéri, *Stability properties of POD-Galerkin approximations for the compressible Navier-Stokes equations*, Theor. Comp. Fluid Dyn. **13** (2000), no. 6, 377–396.
- [10] A. Hay, J.T. Borggaard, and D. Pelletier, *Local improvements to reduced-order models using sensitivity analysis of the proper orthogonal decomposition*, J. Fluid Mech. **629** (2009), 41–72.
- [11] E.A. Christensen, M. Brøns, and J.N. Sørensen, *Evaluation of Proper Orthogonal Decomposition-based decomposition techniques applied to parameter-dependent nonturbulent flows*, SIAM J. Sci. Comput. **21** (1999), no. 4, 1419–1434.
- [12] K. Kunisch and S. Volkwein, *Galerkin Proper Orthogonal Decomposition Methods for a General Equation in Fluid Dynamics*, SIAM J. Numer. Anal. **40** (2003), no. 2, 492–515.
- [13] Z. Wang, I. Akhtar, J. Borggaard, and T. Iliescu, *Proper orthogonal decomposition closure models for turbulent flows: A numerical comparison*, Comput. Meth. Appl. Mech. Engrg. **237–240** (2012), 10–26.
- [14] J.S. Peterson, *The reduced basis method for incompressible viscous flow calculations*, SIAM J. Sci. Stat. Comput. **10** (1989), 777–786.
- [15] K. Veroy and A.T. Patera, *Certified real-time solution of the parametrized steady incompressible Navier-Stokes equations: rigorous reduced-basis a posteriori error bounds*, Int. J. Numer. Meth. Fluids **47(8–9)** (2005), 773–788.
- [16] A. Quarteroni and G. Rozza, *Numerical solution of parametrized Navier-Stokes equations by reduced basis methods*, Numer. Methods Partial Differential Equations **23(4)** (2007), 923–948.
- [17] S. Deparis and G. Rozza, *Reduced basis method for multi-parameter-dependent steady Navier-Stokes equations: Applications to natural convection in a cavity*, J. Comp. Phys. **228** (2009), no. 12, 4359–4378.
- [18] A. Manzoni, *An efficient computational framework for reduced basis approximation and a posteriori error estimation of parametrized Navier-Stokes flows*, ESAIM Math. Modelling Numer. Anal. (2014), 1–27, in press.
- [19] T. Lassila, A. Manzoni, A. Quarteroni, and G. Rozza, *A reduced computational and geometrical framework for inverse problems in hemodynamics*, Int. J. Numer. Meth. Biomed. Engng. **29** (2013), no. 7, 741–776.
- [20] A. Manzoni, A. Quarteroni, and G. Rozza, *Model reduction techniques for fast blood flow simulation in parametrized geometries*, Int. J. Numer. Meth. Biomed. Engng. **28(6–7)** (2012), 604–625.
- [21] J. Baiges, R. Codina, and S. Idelsohn, *Explicit reduced-order models for the stabilized finite element approximation of the incompressible Navier-Stokes equations*, Int. J. Numer. Meth. Fluids **72** (2013), no. 12, 1219–1243.

- [22] D. Chapelle, A. Gariah, P. Moireau, and J. Sainte-Marie, *A Galerkin strategy with Proper Orthogonal Decomposition for parameter-dependent problems – Analysis, assessments and applications to parameter estimation*, ESAIM Math. Modelling Numer. Anal. **47** (2013), no. 6, 1821–1843.
- [23] D. Amsallem and C. Farhat, *On the stability of reduced-order linearized computational fluid dynamics models based on POD and Galerkin projection: descriptor versus non-descriptor forms*, Reduced Order Methods for Modeling and Computational Reduction (A. Quarteroni and G. Rozza, eds.), vol. 9, Springer Milano, MS&A Series, 2013, pp. 215–233.
- [24] I. Akhtar, A. H. Nayfeh, and C. J. Ribbens, *On the stability and extension of reduced-order Galerkin models in incompressible flows*, Theor. Comput. Fluid Dyn. **23** (2009), no. 3, 213–237.
- [25] S. Sirisup and G.E. Karniadakis, *Stability and accuracy of periodic flow solutions obtained by a POD-penalty method*, J. Phys. D **202** (2005), no. 3, 218–237.
- [26] A. Caiazzo, T. Iliescu, V. John, and S. Schyschlowa, *A numerical investigation of velocity-pressure reduced order models for incompressible flows*, J. Comput. Phys. **259** (2014), 598–616.
- [27] G. Rozza and K. Veroy, *On the stability of reduced basis methods for Stokes equations in parametrized domains*, Comput. Meth. Appl. Mech. Engrg. **196** (2007), no. 7, 1244–1260.
- [28] G. Rozza, D.B.P. Huynh, and A. Manzoni, *Reduced basis approximation and a posteriori error estimation for Stokes flows in parametrized geometries: roles of the inf-sup stability constants*, Num. Math. **125** (2013), no. 1, 115–152.
- [29] A. Gerner and K. Veroy, *Certified reduced basis methods for parametrized saddle point problems*, SIAM J. Sci. Comp. **34** (2012), no. 5, A2812–A2836.
- [30] A. Manzoni, A. Quarteroni, and G. Rozza, *Shape optimization for viscous flows by reduced basis methods and free-form deformation*, Int. J. Numer. Meth. Fluids **70** (2012), no. 5, 646–670.
- [31] L. Iapichino, A. Quarteroni, and G. Rozza, *A reduced basis hybrid method for the coupling of parametrized domains represented by fluidic networks*, Comput. Meth. Appl. Mech. Engrg. **221–222** (2012), 63–82.
- [32] M. S. Engelman, G. Strang, and K. J. Bathe, *The application of quasi-Newton methods in fluid mechanics*, Int. J. Numer. Meth. Engng. **17** (1981), no. 5, 707–718.
- [33] M. Barrault, Y. Maday, N.C. Nguyen, and A.T. Patera, *An ‘empirical interpolation’ method: application to efficient reduced-basis discretization of partial differential equations*, C. R. Acad. Sci. Paris. Sér. I Math. **339** (2004), no. 9, 667–672.
- [34] H. Antil, M. Heinkenschloss, and D. Sorensen, *Applications of the discrete empirical interpolation method to reduced order modelling of nonlinear and parametric systems*, Reduced Order Methods for Modeling and Computational Reduction (A. Quarteroni and G. Rozza, eds.), vol. 9, Springer Milano, MS&A Series, 2013, pp. 101–136.
- [35] M.D. Gunzburger, J.S. Peterson, and J.N. Shadid, *Reduced-order modeling of time-dependent PDEs with multiple parameters in the boundary data*, Comput. Meth. Appl. Mech. Engrg. **196** (2007), no. 4–6, 1030 – 1047.
- [36] J. Burkardt, M. Gunzburger, and H.C. Lee, *POD and CVT-based reduced-order modeling of Navier-Stokes flows*, Comput. Meth. Appl. Mech. Engrg. **196** (2006), no. 1-3, 337–355.
- [37] A. Quarteroni, *Numerical models for differential problems*, Modeling, Simulation and Applications (MS&A), vol. 8, Springer-Verlag Italia, Milano, 2014.
- [38] A. Quarteroni, G. Rozza, and A. Manzoni, *Certified reduced basis approximation for parametrized partial differential equations in industrial applications*, J. Math. Ind. **1** (2011), no. 3, 1–49.
- [39] D. Xiao, F. Fang, A.G. Buchan, C.C. Pain, I.M. Navon, J. Du, and G. Hu, *Non-linear model reduction for the Navier-Stokes equations using the residual DEIM method*, J. Comp. Phys. **263** (2014), 1–18.
- [40] K. Carlberg, C. Farhat, J. Cortial, and D. Amsallem, *The GNAT method for nonlinear model reduction: effective implementation and application to computational fluid dynamics and turbulent flows*, J. Comp. Phys. **242** (2013), 623–647.
- [41] K. Carlberg, C. Bou-Mosleh, and C. Farhat, *Efficient non-linear model reduction via a least-squares Petrov-Galerkin projection and compressive tensor approximations*, Int. J. Numer. Meth. Engng. **86** (2011), no. 2, 155–181.
- [42] F. Brezzi and K.J. Bathe, *A discourse on the stability conditions for mixed finite element formulations*, Comput. Meth. Appl. Mech. Engrg. **82** (1990), no. 1–3, 27–57.
- [43] D. Boffi, F. Brezzi, and M. Fortin, *Mixed finite elements and applications*, Springer-Verlag Berlin-Heidelberg, 2013.
- [44] H.C. Elman, D.J. Silvester, and A.J. Wathen, *Finite elements and fast iterative solvers: With applications in incompressible fluid dynamics*, Numerical Mathematics and Scientific Computation, OUP Oxford, 2005.
- [45] D. Chapelle and K.J. Bathe, *The inf-sup test*, Computers & Structures **47** (1993), no. 4-5, 537–545.
- [46] K.J. Bathe, *The inf-sup condition and its evaluation for mixed finite element methods*, Computers & Structures **79** (2001), no. 2, 243–252.
- [47] P. Jr. Ciarlet, *T-coercivity: application to the discretization of Helmholtz-like problems*, Computers & Mathematics with Applications **64** (2012), no. 1, 22–34.

- [48] L. Chesnel and P. Jr. Ciarlet, *T-coercivity and continuous Galerkin methods: application to transmission problems with sign changing coefficients*, Num. Math. **124** (2013), no. 1, 1–29.
- [49] D.S. Malkus, *Eigenproblems associated with the discrete LBB condition for incompressible finite elements*, Int. J. Engng. Sci. **19** (1981), no. 10, 1299–1310.
- [50] D.J. Knezevic and J.W. Peterson, *A high-performance parallel implementation of the certified reduced basis method*, Comput. Meth. Appl. Mech. Eng. **200** (2011), no. 13–16, 1455–1466.
- [51] B.S. Kirk, J.W. Peterson, R.H. Stogner, and G.F. Carey, *libMesh: a C++ library for parallel adaptive mesh refinement/coarsening simulations*, Eng. Comput. **22** (2006), no. 3–4, 237–254.

# MOX Technical Reports, last issues

Dipartimento di Matematica “F. Brioschi”,  
Politecnico di Milano, Via Bonardi 9 - 20133 Milano (Italy)

- 13/2014** BALLARIN, F.; MANZONI, A.; QUATERONI, A.; ROZZA, G.  
*Supremizer stabilization of POD-Galerkin approximation of parametrized Navier-Stokes equations*
- 12/2014** FUMAGALLI, I; PAROLINI, N.; VERANI, M.  
*Shape optimization for Stokes flow: a reference domain approach*
- 11/2014** TADDEI, T.; QUATERONI, A.; SALSA, S.  
*An offline-online Riemann solver for one-dimensional systems of conservation laws*
- 10/2014** ANTONIETTI, P.F.; DEDNER, A.; MADHAVAN, P.; STANGALINO, S.; STINNER, B.; VERANI, M.  
*High order discontinuous Galerkin methods on surfaces*
- 09/2014** CHEN, P.; QUATERONI, A.  
*A new algorithm for high-dimensional uncertainty quantification problems based on dimension-adaptive and reduced basis methods*
- 08/2014** CATTANEO, L; ZUNINO, P.  
*A computational model of drug delivery through microcirculation to compare different tumor treatments*
- 07/2014** AGASISTI, T.; IEVA, F.; PAGANONI, A.M.  
*Heterogeneity, school-effects and achievement gaps across Italian regions: further evidence from statistical modeling*
- 06/2014** BENZI, M.; DEPARIS, S.; GRANDPERRIN, G.; QUATERONI, A.  
*Parameter estimates for the relaxed dimensional factorization preconditioner and application to hemodynamics*
- 05/2014** ROZZA, G.; KOSHAKJI, A.; QUATERONI, A.  
*Free Form Deformation Techniques Applied to 3D Shape Optimization Problems*
- 04/2014** PALAMARA, S.; VERGARA, C.; CATANZARITI, D.; FAGGIANO, E.; CENTONZE, M.; PANGRAZZI, C.; MAINES, M.; QUATERONI, A.  
*Patient-specific generation of the Purkinje network driven by clinical measurements: The case of pathological propagations*